



Climate, African and Beringian subaerial continental shelves, and migration of early peoples

Renée Hetherington^{a,*}, Edward Wiebe^a, Andrew J. Weaver^a, Shannon L. Carto^b,
Michael Eby^a, Roger MacLeod^c

^a*School of Earth and Ocean Sciences, University of Victoria, P.O. Box 3055 STN CSC, Victoria, BC, Canada V8W 3P6*

^b*Natural Resources Canada, Geological Survey of Canada, 9860 West Saanich Road, P.O. Box 6000, Sidney, BC, Canada V8L 4B2*

^c*Geology, University of Toronto, 1265 Military Trail, Toronto, Ont., Canada M1C1A4*

Abstract

The impacts of rapid climate change likely influenced human behaviour during the last glacial cycle, potentially stimulating habitation of, and migration along, continental shelves exposed during periods of lowered sea level. Last glacial maximum (LGM) climate model simulation shows cooler surface air temperatures in Eastern Beringia than Western and Central Beringia. Central Beringia was slightly wetter than present day (PD), whereas Eastern and Western Beringia were drier than PD. However Eastern Beringia was wetter than either Central or Western Beringia. Increased C3 grass coverage is shown in Eastern and Western Beringia, but increased C3 grass net primary productivity (NPP) appears only in Western Beringia; needleleaf trees and many shrubs disappear, replaced by barren soil and C3 grass. Such change would have squeezed species dependant on needleleaf trees out of Western and Eastern Beringia and potentially initiated their migration to more southerly parts of East Asia where a diminishing needleleaf tree environment remained. Shrub-reliant species in Eastern and Western Beringia and C3 grass-dependant species in East Asia and Eastern Beringia would have found additional and productive habitat on the subaerial continental shelf.

The LGM simulation identifies cooler LGM temperatures and increased aridity in South and particularly Central Africa, and associated large reductions in LGM broadleaf tree NPP and coverage in Africa, reduced C3 grass NPP particularly in Central Africa, decreased needleleaf tree NPP in South Africa, reduced shrub coverage in North and Central Africa, and greater barren ground coverage in Central and South Africa. Reduced productivity and shifting vegetation during the LGM may have squeezed flora, fauna, and human populations onto the potentially more productive and proximally located exposed continental shelf.

© 2007 Elsevier Ltd and INQUA. All rights reserved.

1. Introduction

The purpose of this paper is to review the archaeological evidence of key human dispersals throughout the history of the peopling of the world and relate it to climate during the last glacial cycle (LGC). Emphasis will be placed on the relevance of the extensive continental shelves of the Bering and Chukchi Seas, which when exposed by lowered sea level during the last glacial maximum (LGM) formed part of the region known as Beringia. Beringia extended from northeastern Siberia to the MacKenzie River in the Yukon of Canada and is the region through which, many theorize, early people migrated when first peopling the Americas.

We will also briefly examine Africa and its surrounding continental shelf, which was the focus of research by Faure et al. (2002) in the application of their *Coastal Oasis* model. We compare the equilibrium climates computed by the University of Victoria (UVic) Earth system climate model (ESCM) using both LGM and present day (PD) forcing in order to better understand the impact of climate on human migration along these shelves during the LGM. We provide insights into the importance of understanding the continental shelf environment and its influence on human migration, particularly during periods of rapid climate change when slow, gradual adaptation to a changing environment was not a viable alternative for early peoples.

Climate has affected, and continues to critically influence, the success of civilizations and the livelihood and economic well being of peoples around the world. Rapid environmental

*Corresponding author.

E-mail address: reneehet@ocean.seos.uvic.ca (R. Hetherington).

changes frequently generate rapid behavioural responses by humans living in affected regions. Detrimental environmental change can result in temporary abandonment of home territories. As detrimental environmental change expands within a region, whether through increased desertification, cooling, or an increase in extreme events, and also when human populations expand, reduction in available resources frequently results in shifts in resource usage. Persistent change that causes the destruction of the original living environment will typically lead to permanent relocation of the surviving populace. As subsistence resources in new territories also become limited, people will inevitably be required to travel farther afield to find suitable new habitation territories, stimulating mass migrations.

Such was likely the case during the LGC, which began 135,000 years ago (ka). Transitions between cool climate intervals (stadials) and warm intervals (interstadials), which lasted hundreds to thousands of years (Dansgaard et al., 1984; Oeschger et al., 1984), were rapid. The strength of Atlantic thermohaline circulation, which directly influences Northern Hemisphere climate, was highly variable (see Weaver (2004) for a review). In response, vegetation and faunal species' distribution changed both significantly and rapidly. Global sea level fell and rose resulting in the exposure and subsequent inundation of continental shelves. It was during this time of highly variable climate, when the coastlines of the world were expanding and contracting in response to eustatic and isostatic sea-level changes that the most pervasive expansion of *Homo sapiens* occurred.

Many anthropological theories explaining human migrations during the LGC invoke climate change as a determinant and cite migration paths utilizing in part, or exclusively, subaerial continental shelves. However, many theories remain just that, lacking substantive support; what evidence that may exist is drowned or has been washed away through marine erosion. Thus, the location, extent, and timing of exposure of the world's continental shelves are important scientific data that when available, assist in determining the location of ancient shorelines and the timing and feasibility of potential migration routes. Route feasibility is further dependant upon the suitability of subaerial continental shelf environments as migration corridors through which, and along which, early people may have lived and journeyed. For example, habitation of high-latitude continental shelves would have been restricted when shelves were covered with glacial ice; alternatively, when ice-free they may have served as productive glacial refugia (see for example, Hetherington et al., 2003); in desiccated tropical or subtropical arid lands subaerial continental shelves may have acted as "coastal oases" during periods of severe climate stress (Faure et al., 2002).

Unfortunately our understanding of the local and regional sea-level histories of relevant continental shelves and their environments around the world is limited. In addition to changing sea level, shelf environments were affected by changes in sea-ice cover (e.g., Ganopolski et al.,

1998; Braconnot et al., 1999; Vavrus, 1999) and the albedo of land surface resulting from fluctuating snow cover (Bonan et al., 1992; Foley et al., 1994; Berger, 2001). Although global eustatic sea-level curves continue to be developed and refined (see for instance, Lambeck et al., 2002; Cutler et al., 2003), they remain limited in their regional application especially in far-field, tectonically active, and high-latitude regions where glacio-isostatic responses have resulted in disparate sea-level curves for locally proximal sites (see for example, Hetherington and Barrie, 2004; Hetherington et al., 2004). When environmental proxy data are sparse and/or contradictory, ESCMs can be used to elucidate global and regional climate and vegetation characteristics.

Most climate models do not include interactive dynamical ice sheets and must instead reply upon reconstructions of glacial ice thickness and extent as a specified land-surface boundary condition. Such ice sheet reconstructions have been developed for the LGM to the PD (e.g., Peltier, 2004), however the modelling of earlier intervals remains a challenge. Recent proxy and field data-based global digital glacial ice extent compilations of Ehlers and Gibbard (2004a–c) provide a new basis for calculating LGC glacial ice extent. If we are to shed light on the viability of subaerial continental shelves as corridors used by migrating early peoples during the LGC, both climate modelling and proxy data will be necessary to elucidate the environmental and climatological characteristics of continental shelves and their surrounding regions.

2. Archaeological setting

Some of the uniqueness that distinguishes modern humans from other species is the result of genetic adaptation, while some is the result of developmental, behavioural and physiological adaptability. However, this distinction is not always recognized. According to neo-Darwinists, genetic adaptation is improved fitness to environment that results from the natural selection of beneficial gene mutations. It is slow to respond to environmental change; whereas developmental, behavioural and physiological adaptability can respond rapidly to sudden climate change. During periods of climate stability the importance of this distinction may not have been particularly noticeable or relevant to our species, but during periods of rapid climate change, adaptability was the characteristic that provided humans an opportunity to respond quickly. One mechanism of behavioural adaptability is the capacity to disperse or migrate. Hominins first dispersed out of Africa nearly 2 million years ago (Ma), but it was during the highly variable climatic period of the LGC that a new species of hominin-*H. sapiens*—embarked on a series of rapid and extensive migrations that resulted in their populating both the Old and the New World.

The first hominin dispersals occurred out of Africa in what seem to have been multiple waves, including an initial dispersal of *Homo erectus* (sensu stricto) to Java, Indonesia

before 1.5 Ma and perhaps as early as 1.9 Ma (Aguirre and Carbonell, 2001; Larick et al., 2001; although see Langbroek and Roebroeks, 2000; Sémah et al., 2000). A second dispersal, which reached Dmanisi, Georgia, of hominins possessing progressive “modern” traits occurred by ~ 1.7 Ma if not before (Gabunia et al., 2000, 2001; Aguirre and Carbonell, 2001). A third migration out of Africa has been suggested for the Ubeidiya hominin remains associated with the Acheulean toolkit located in the Jordan Valley, Israel and dated to ca. 1.5 Ma (Tchernov, 1992; Bar-Yosef, 1994; Belmaker et al., 2002). A fourth more recent dispersal out of Africa and into Europe, evidenced most notably at the Atapuerca-Gran Dolina site in north-central Spain with the presence of *H. antecessor*, intermediate between *H. erectus* and *H. ergaster* and modern humans, potentially implies dispersal out of Africa at ~ 900 ka (de Castro et al., 2004). Whereas earlier hominins may not have left Africa via the Strait of Gibraltar, the Atapuerca discovery raises this possibility for mid-Middle Pleistocene dispersals (Aguirre and Carbonell, 2001). These early human dispersals set the stage for the later and far more pervasive expansion of *H. sapiens*.

H. sapiens first appeared prior to the onset of the LGC and subsequently migrated around the world. Geneticists, using mutation rates to set the human “molecular clock”, suggest that modern humans are the descendants of an ancestral African population living between 100 and 200 ka (Bräuer, 1989; Stringer, 1989, 1990; Balter, 2002). Fossil experts are generally in agreement, basing their interpretation on the 130,000-year-old skeleton found at Omo Kibish in Ethiopia and the 100,000-year-old fossils from Klasies River Mouth, South Africa. Archaeological and human mtDNA evidence suggests a rapid migration of *H. sapiens* out of Africa into the Middle East (Valladas et al., 1988) and Asia at around 100 ka followed by an extended period of in-situ diversification and restricted migration (Endicott et al., 2004), although others disagree with this timing (see for example, McBrearty and Brooks, 2000). Recently discovered artifacts dating to approximately 125 ka found on the Red Sea coast of Eritrea imply early human occupation of coastal areas and exploitation of near-shore marine food resources in East Africa (Walter et al., 2004) and may suggest an early expansion out of Africa and into Southeast Asia along the subaerial continental shelf.

Interestingly, the Red Sea find dates to ~ 125 ka when, although sea levels were very similar to today, the region had just experienced a period of rapid sea-level change. Global eustatic sea level rose rapidly (~ 120 m according to Lambeck et al., 2002) between 140 and 135 ka and then subsequently fell rapidly (~ 60 m according to Lambeck et al., 2002) between about 135 ka and about 130 ka. After 130 ka, rapidly rising sea levels inundated subaerial continental shelves. By 125 ka, shelves previously exposed to a depth of as much as 100 m were inundated as sea levels reached ~ 6 m above PD levels.

Occupation of Australia occurred by about 55 ka ago (Roberts et al., 1990, 1994) or more conservatively between

45 and 42 ka ago for both Australia and the Huon Peninsula, New Guinea (O’Connell and Allen, 2004) when sea level was between 45 and 60 m lower than today (Lambeck et al., 2002) exposing portions of the Sunda and Australian shelves. The earliest modern human fossils in Europe date to 36.3 thousand radiocarbon years before present (^{14}C ka BP; 41.5 ka) in Hahnöfersand, Germany (Hublin, 2000) and between ~ 34.0 and 36.0 ^{14}C ka BP (39.2 and 41.4 ka) in southwestern Romania (Trinkaus and Duarte, 2003) and overlap with Neanderthal populations until the disappearance of the latter at ~ 24.5 ^{14}C ka BP (29.1 ka; Duarte et al., 1999). According to the Clovis First hypothesis, occupation of the Americas occurred between 11.0 and 12.0 ^{14}C ka BP (12.9 and 13.9 ka) when lowered sea levels exposed the Beringian continental shelf between northeast Asia and what is now Alaska. Alternatively, the coastal migration hypothesis suggests that people migrated along the southern edge of the exposed Beringian shelf and down the Pacific coasts of North and South America. In addition to these theories, new fossil, DNA, craniometric, and other archaeological research suggests earlier contact with the Americas and/or colonizations originating in regions other than northeast Asia, including potentially Europe, Australia, Polynesia, and Africa (Holden, 1999; Neves et al., 1999; González-José et al., 2003).

Although many human migration theories imply the use of subaerial continental shelves, the archaeological record, particularly that relevant to coastal adaptations and the use of boating technology, is likely seriously underrepresented because of the rapidly changing sea-level history of shelf environments (Erlandson, 2002). Although research is ongoing to map the LGC sea-level history and environment of continental shelves around the world (e.g., IGCP Project 464, 2001–2006), there are many regions where data and/or research are insufficient to provide a meaningful history. Thus new data and additional research techniques, including the use of comprehensive climate models, are useful in providing the climatic and environmental information necessary for revealing the relevance of subaerial continental shelves to human migration during the LGC.

3. Last glacial cycle climate

At the onset of the last interglacial (135 ka), atmospheric carbon dioxide (CO_2) and methane (CH_4) levels were rising rapidly in association with an increase in surface-air temperature. Global eustatic sea level, which according to Lambeck et al. (2002) was ~ 130 m below PD levels at 140 ka, rose more than 110 m over a 5000-year interval before falling dramatically to ~ 80 m below PD levels at 130 ka (Lambeck et al., 2002; Fig. 1a). At ~ 130 ka an extremely rapid rise in sea level ensued, whereby sea level rose to ~ 6 m above present sea level within a matter of a few thousand years (Ku et al., 1974; Lambeck et al., 2002; Cutler et al., 2003). During the Eemian interglacial period

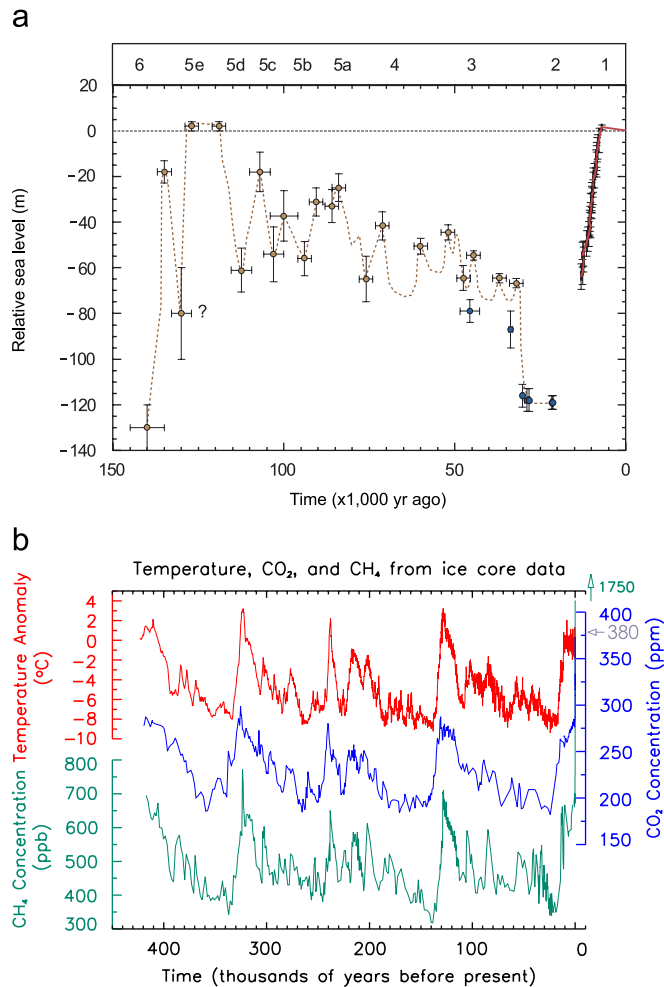


Fig. 1. Relative sea level for the last glacial cycle and four glacial cycles recorded in the Vostok ice core: (a) the relative sea-level curve for the last glacial cycle. Error bars define the upper and lower limits. The main oxygen isotope stages MIS-6 to MIS-1, including substages are identified. Reprinted by permission from Macmillan Publishers Ltd: Nature (Lambeck et al., 2002), copyright 2005; (b) Variations in local Antarctic atmospheric temperature, as derived from oxygen isotope data, as well as concentrations of atmospheric CO₂ and CH₄ from Vostok, Antarctica ice core records. Blue arrow refers to present day carbon dioxide (CO₂) concentration of 380 ppm; green arrow refers to present day methane (CH₄) concentration of 1750 ppb. Modified from Petit et al. (1999).

(oxygen isotope stage (OIS) 5e; 135–118 ka) the Earth's globally and annually averaged surface air temperature (SAT) was up to 2 °C warmer than preindustrial times (White, 1993). Between 118 and 110 ka, rapid cooling resulted in a sudden drop, between 50 and 80 m, in glacio-eustatic sea level (Yoshimori et al., 2002; see also Lambeck et al., 2002; Cutler et al., 2003). By 116 ka glacial inception had begun (Imbrie et al., 1984). CO₂ and CH₄ levels continued to fall along with atmospheric temperature (Fig. 1b). Cutler et al. (2003) inferred an ~40 m drop in sea level over 10,000 years; sea level dropped by 57 m by 92.6 ka after which sea level rose more than 40 m in the subsequent 10,000-year interval.

The last glaciation evolved progressively into the full glacial, known as the Lower Pleniglacial (OIS 4), between 75 and 60 ka. Sea level fell up to 60 m over a 6000-year interval between about 76 and 70 ka (Cutler et al., 2003). It was after reaching this cold and dry low point that OIS 3 (60–25 ka) began and the climate became highly unstable, but generally cooler and drier than at present. Sea level oscillated between 60 m (Lambeck et al., 2002) and 80 m (Cutler et al., 2003) below PD levels until around 35 ka when sea levels fell to approximately 120 m below today's level as glacial ice reached its maximum global extent at the LGM (21.4 ka; 18.0 ¹⁴C ka BP; Fairbanks, 1989). High amplitude millennial-timescale variability between warm (interstadial) and cold (stadial) states, known as Dansgaard–Oeschger (D–O) oscillations were a prominent feature of the LGC (Dansgaard et al., 1993; Bond et al., 1997; Schulz et al., 2002). D–O oscillation transitions were associated with local mean surface-air temperature changes over Greenland of up to 10 °C occurring on decadal timescale (e.g., Lang et al., 1999). However, the effects of D–O oscillations were not local (Justino, 2004); evidence for a global impact has been found in the North Pacific (Kotilainen and Shackleton, 1995), the Santa Barbara Basin (Kennett and Ingram, 1995; Behl and Kennett, 1996), South America (Lowell et al., 1995), the Arabian Sea (Schulz et al., 1998), and the South China Sea (Wang, 1999). Furthermore, there is an out-of-phase climate response between the Northern and Southern hemispheres that creates a bipolar seesaw effect. Thus, during stadial phases of D–O oscillations, when the northern Atlantic Ocean was cool, the southern Atlantic Ocean was warm, and during interstadial phases when the northern Atlantic Ocean was warm, the southern Atlantic Ocean was cool (e.g., Crowley, 1992; Stocker, 1998; Schmittner et al., 2003).

During the transition from the LGM to the Holocene, more specifically, at 14.6 ka, the Bølling–Allerød interstadial event occurred. A large increase in the strength of the Atlantic thermohaline circulation was responsible for a 150 per mil decrease in atmospheric radiocarbon and a 3 °C increase in annual mean sea-surface temperature over ~500 years (Weaver et al., 2003). This event marked the termination of the last glacial period. Subsequent to the LGM glacio-eustatic sea level began another rapid rise; during one interval it rose 20 m in less than 500 years (Fairbanks, 1989); air temperature warmed to near-interglacial levels and continental ice sheets retreated significantly. Then within a few decades North Atlantic warming was interrupted by the last known D–O event—the Younger Dryas (sometimes also called Heinrich Event 0 [H0])—between 12.7 and 11.7 ka, an abrupt, brief cold interval during which sea-surface temperatures in the Atlantic dropped by several degrees (Dansgaard et al., 1989). The Younger Dryas terminated suddenly, within a few decades, setting the stage for the onset of the Holocene, a period of remarkable relative climate stability (Weaver, 2004).

3.1. Beringia climate during the LGM

The relevance of the Beringian continental shelf to the peopling of the Americas is restricted to the period during or just subsequent to the LGM. Prior to this time it is generally, though not universally, thought that humans did not inhabit the Americas. The region thus provides an important test case for the application of climate modelling and proxy data analysis to subaerial continental shelves and theories of human migration.

The character of the Beringian landscape during and subsequent to the LGM has been an issue of scientific debate over recent decades. Limited and disparate data has resulted in contradictory interpretations on both sides of Beringia and generated the *productivity paradox* in which late Pleistocene megafauna appeared to have successfully survived on what appeared to be the limited biomass productivity capacity of tundra vegetation (see, Hopkins et al., 1982). The sea-level history is uncertain; despite ongoing research, there currently exists little substantive evidence regarding the environment and history of exposure and inundation of Beringia. Although global glacio-eustatic sea-level curves have been used to ascertain the sea-level history and palaeogeography of the region (Manley, 2002), it is clear that local sea levels vary temporally and spatially as a result of glacial and hydrostatic adjustments as well as tectonic effects (Mackey et al., 1997).

Glacial ice extent has also been an issue of substantial controversy. Early interpretations had ice extending over much of Western Beringia (Grosswald, 1988, 1998; Grosswald and Hughes, 1995, 2002). However a growing body of new data, supported by modelling studies, suggest restricted moisture in northern Russia during the LGM (Siegert and Marsiat, 2000; Siegert et al., 2001), and far more limited ice coverage (Svendsen et al., 1999) with ice restricted to valleys and cirques in local mountain ranges (Brigham-Grette et al., 2004). Much of Eastern Beringia was ice-free during the LGM with the exception of southern Alaska, southern Yukon, and west of the coast and St. Elias Mountains (Clague et al., 2004).

Extensive sea-ice cover in the Bering Sea and along the Arctic Ocean coast of the Bering land bridge added to the continental climate of Western Beringia (Brigham-Grette et al., 2004); yet sufficiently productive vegetation persisted to provide enough biomass to support megafauna throughout much of the LGM to Holocene interval (Vartanyan et al., 1993; Brigham-Grette et al., 2004). Local variations such as those suggested by Yurtsev (2001) where two disparate habitat regions collide, for instance where arid plains meet mountain glaciers, resulted in enhanced productivity that may have provided habitats conducive to megafaunal survival.

Interpretations about the climate and vegetation across the region also differ. Some researchers suggest that whereas Western and Eastern Beringia appear to have been dry grassland during the LGM, Central Beringia

possessed a moister, more tundra-like environment (e.g., Barnosky et al., 1987; Hamilton et al., 1993; Anderson and Brubaker, 1994; Elias et al., 1996; Guthrie, 2001; Brigham-Grette et al., 2004). Clague et al. (2004) suggest that the persistence of high-pressure systems prevented moisture from reaching much of Eastern Beringia, maintaining aridity in the region; evaporation likely exceeded precipitation in lake basins, further enhancing aridity. Based on Alaskan lake levels Barber and Finney (2000) proposed precipitation was 40–75% less than occurs today. Using pollen and plant macrofossil evidence in cores obtained from the Chuchki and Bering Seas, Elias et al. (1996, 1997) infer that mesic herb–shrub tundra covered much of the Bering landbridge. However, others have suggested that although the herb–shrub tundra may have appeared earlier, during the later stages of the last glacial interval, a drier climate resulted in a herb-dominated tundra vegetation in central and Eastern Beringia. Guthrie (2001) argued that because Central Beringia was more maritime than either Western or Eastern Beringia, it possessed greater cloud cover, generating more mesic vegetation that caused Central Beringia to behave like a filter to some steppe-adapted species including perhaps the woolly rhino, camels, and short-faced bears. Additional research based on insect remains from Eastern Beringia indicates mean summer temperatures only 1–4 °C cooler than today, in sharp contrast to estimates for LGM faunas south of the Laurentide ice sheets which were 10–19 °C colder than modern (Elias, 2001).

Vegetation modelling by Kaplan (2001) and Kaplan et al. (2003) suggests greatly reduced low- and high-shrub tundra in Beringia during the LGM and greater simulated extent of graminoid and forb tundra and is consistent with that based on paleoenvironmental data by Bigelow et al. (2003). However, Kaplan adds a caveat that the LGM model simulations assumed the presence of the East Siberian Ice sheet, which as stated above, is now deemed not to have existed during the LGM. Kaplan (2001) attributes the productivity paradox to greater productivity of the more extensive graminoid and forb tundra biome during the LGM; increased solar radiation resulted in the biome growing at lower latitudes during the LGM than it does today and reduced cloudiness facilitated increased photosynthesis.

3.2. Africa

Previous reconstructions of the African paleoclimate, during and subsequent to the LGM, have been severely limited by poor instrumental paleoclimate records. However, an expanding understanding of vegetation dynamics and aeolian sediment activity during the LGM, is improving our ability to objectively quantify climate change and variability in Africa, as well as to ascertain the manifestation of global climate events on a regional scale in Africa. In this study, we focus on African climate during the LGM as a first step in efforts to improve our ability to model

earlier intervals during the LGC when hominins migrated out of Africa—repeatedly.

3.2.1. North Africa

In North Africa and the Levant (Fig. 2), prior to the LGM, at around 28.0–25.0 ^{14}C ka BP (ca. 32.7–30.0 ka), conditions appear to have been significantly moister than at present permitting the formation of soils (Goodfriend and Margaritz, 1988). In contrast, the LGM appears to have been a period of increased aridity marked by sand mobilization in the whole Sahara–Sahel region (Swezey, 2001). Palaeohydrological records collected from across the Sahara indicate that lake levels in this region were significantly reduced during the LGM, including the Lake Chad Basin where extremely low lake levels facilitated the persistence of semi-desert grasslands (Maley, 1977; Servant and Servant-Vildary, 1980), Crater Lake in Nigeria (Salzmann et al., 2002), and Jebel Marra Crater Lake in Northeast Africa (Williams et al., 1980). Ancient sand dune distributions suggest that desert conditions in North Africa expanded farther to the south than today; although the north-west corner of the Sahara appears to have been somewhat moister than today, with a belt of semi-desert appearing to the south of the PD desert margin (Hooghiemstra et al., 1992). During the LGM it is estimated that the southern desert boundary was situated 5° farther south than at present (Thomas and Thorp, 1995), and that the Saharan–Sahelian boundary reached as far south as 14°N in Senegal and 12°N in East Nigeria (Rossignol-Strick and Duzer, 1979; Dupont and Hooghiemstra, 1989; Volkel, 1989; Lézine, 1991). Two pollen localities, one in northern Israel and the other in northern Lebanon, which presently

support a moister-climate closed forest, during the LGM seem to have supported a band of open woodland or forest-steppe along the coast that reached perhaps 50 km inland (Goodfriend and Margaritz, 1988). Marine pollen records from the Atlantic coast (Hooghiemstra et al., 1992; Dupont, 1993) and the Gulf of Gabes (Brun, 1991) show that the hyper-arid climatic conditions of the LGM terminated between ca. 13.0 and 12.0 ^{14}C ka BP (ca. 15.4 and 13.9 ka) with the spread southward of Mediterranean vegetation. Nevertheless, it is contended that the overall climate in Africa remained relatively dry until the onset of the Holocene (Hoelzmann et al., 2004).

3.2.2. Central Africa

Conditions in the central African forest region, prior to the LGM, (28.0–25.0 ^{14}C ka BP; ca. 32.7–26.5 ka), are thought to have been significantly cooler than at present, although not as cold as they later became during the LGM (Giresse and Le Ribault, 1990). During the LGM, the present-day rainforest region of central and western Africa is documented to have experienced a reduction in forest area due to the apparent cooling of the continent. Analysis of two pollen sequences recovered from Lake Barombi and Ngamakala Pond in southern Cameroon and southern Congo, respectively, imply semi-deciduous forests and grasslands prevailed at these sites during the LGM (Elenga et al., 1994; Maley and Brenac, 1998). Furthermore, marine pollen records from the eastern Atlantic Ocean indicate a large reduction, although not complete disappearance, in rainforest in West and Atlantic Equatorial Africa during the cold stages (Bengo and Maley, 1991; Lézine and Vergnaud-Grazzini, 1993; Jahns, 1996; Dupont et al., 1998; Jahns et al., 1998). A decrease in temperature in inter-tropical Africa estimated to range between 3 and 8°C was required to produce the observed vegetation shift (Maley, 1981, 1989, 1991, 1996; Maley and Livingstone, 1983). The fragmented forest areas that remained in this region contained a significant proportion of montane trees, implying lowland tropical mean temperatures about 5 – 6°C cooler than at present (Maley, 1989; Livingstone, 1993). Evidence recovered from five pollen sites from the highlands along the eastern edge of the Rift Valley reveal that these vegetation shifts were not restricted to central Africa, but also extended into East Africa (Jolly et al., 1998). The pollen data imply that in areas presently supporting moist forest cover, dry grassland and ericaceous shrub vegetation dominated during the LGM (Jolly et al., 1998).

3.2.3. South Africa

According to oxygen isotope records at Cango Cave, in South Africa and biogenic silica in lake cores in Southeast Africa, the climate during the LGM was cooler, drier, and windier than today; with mean annual temperatures about 5°C cooler than today (Deacon and Deacon, 1999; Farrera et al., 1999; Johnson et al., 2002). Although various lakes in south-central Africa suggest conditions were moister

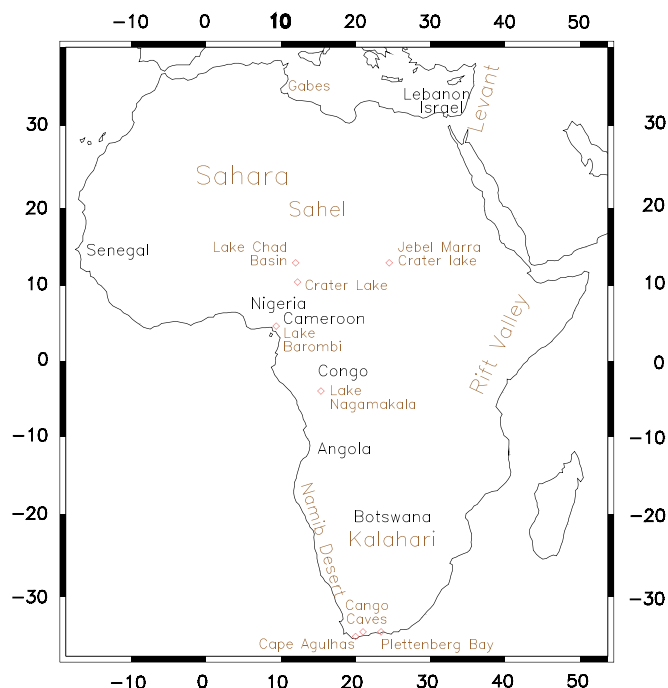


Fig. 2. Map of Africa identifying key locations.

than at present (Brook et al., 1987) and terrigenous sediments in southeast Atlantic Ocean cores imply relative humidity in southwestern Africa during the last glacial interval (Stuut et al., 2002), Lake Malawi in southeastern Africa indicates drier conditions than today (Johnson et al., 2002). Further, pollen and dune evidence from across the region suggests that the LGM was drier than at present. The high ratio of illite clays and plant phytoliths evident in the glacial-age sediments off the coast of northern Angola (Jansen, 1990) implies that the Namibian desert was even drier than at present, and possibly expanded in areal coverage, both eastwards and northwards (Deacon and Lancaster, 1988). Studies conducted on the ancient history of linear dune activity in Botswana and Southeast Namibian desert, revealed that desert conditions were widespread in this area between about 19°S and 17°S and between 24°E and 25°E; an area that presently receives almost 800 mm/yr rainfall and has scrub and woodland vegetation (Stokes et al., 1997). Pollen evidence indicates that in much of central and eastern South Africa, where shrubby karoo or woodland vegetation now predominates, a drier semi-desert karroid scrub seems to have been present (Deacon and Lancaster, 1988; Deacon, 1990). More recently, Elenga et al. (2000) suggest that during the LGM southern African forest and xerophytic woods/scrub were replaced by steppe. Reconstructions of biomes during the LGM indicate that beyond 13°S the western half of southern Africa was desert, with xerophytic woodland occupying much of the remainder; the upland areas carried steppe vegetation (Partridge et al., 1999).

4. Materials and methods

The UVic ESCM was used to compute equilibrium climates for the PD and the LGM. The UVic ESCM consists of a three-dimensional (3D) ocean general circulation model coupled to a dynamic-thermodynamic sea-ice model, an ocean carbon cycle model, a dynamic energy–moisture balance atmosphere model, a land surface model, and a terrestrial vegetation and carbon cycle model (Weaver et al., 2001; Ewen et al., 2003; Matthews et al., 2003a, b; Meissner et al., 2003). A reduced complexity atmosphere model was used for computational efficiency. The atmospheric model includes a parametrization of the water vapour/planetary longwave feedback, while the radiative forcing associated with atmospheric CO₂ changes is externally imposed as a reduction of the planetary long wave radiative flux. A specified lapse rate was used to reduce the land-surface temperature where there is topography. The UVic ESCM has been extensively and successfully evaluated against both contemporary observations (Weaver et al., 2001) and paleo-proxy records (Weaver et al., 1998; Schmittner et al., 2002; Meissner et al., 2003).

The PD model simulation was integrated to equilibrium with orbital, CO₂, and ice sheet forcing specified for the year 1850. The model was then further integrated to the

year 2000 using observed levels of CO₂. This was the PD climate state used to compare with the LGM model and as the base state from which LGM wind anomalies were calculated as in Weaver et al. (2001).

The ice extent and ice height in the LGM simulation was specified according to Peltier's (2004) ICE-5G model. The LGM model simulation was forced using orbital parameters and atmospheric CO₂ for the LGM (200 ppm). LGM sea level was lowered by 120 m. Simulations were integrated to equilibrium under constant forcing for 3000 years with a resolution of 1.8° (latitude) by 3.6° (longitude).

The assessment of regional impacts was based on model simulations pertaining to the regions identified in Fig. 3. For the purpose of this paper we focus on regions relating to (1) Beringia: East Asia, Western Beringia, Eastern Beringia, Canada, and the North Pacific, and (2) Africa: South, Central, and North Africa, Southwest Asia, and India, as well as the North Atlantic Ocean.

5. Results and discussion

5.1. Global interpretations

Figs. 4a–d illustrate the PD and PD minus LGM simulated climate anomalies for global surface air temperatures (SAT) and global precipitation (P). As depicted in Table 1, reduced global P (by 56 mm/yr) and global SATs (by 4 °C) relative to PD resulted in a large increase in modelled global C4 grass coverage (FRAC) and average net primary productivity (NPP) during the LGM combined with substantial reductions in global average NPP of broadleaf (see Figs. 4e and f), needleleaf trees, C3 grass, and, to a lesser extent, shrubs relative to PD. The direction and degree of relative change in LGM vegetation coverage compared with PD does not always coincide with NPP changes. Model simulations show that global average coverage was reduced for broadleaf trees and needleleaf trees (Fig. 5a), and expanded for C3 and C4 grasses (Fig. 5b) and shrubs in the LGM simulation relative to PD (Table 1). This is despite a reduction in global average NPP of C3 grass and shrubs in the LGM simulation. Thus, C4 grass is the only modelled vegetation type which both increased in global average NPP and expanded in global coverage in the LGM simulation. Global average coverage of barren soil in the LGM simulation was also reduced (Fig. 5c and Table 1); this is particularly evident in central southwestern Asia and northwestern Africa.

5.2. Regional interpretations

Regional analysis of model simulations provides some understanding as to how LGM climatic changes may have influenced early peoples and particularly their migration along, and habitation of, subaerial continental shelves. To clarify regional climatic impacts we have shown the LGM climate anomalies relative to PD by region for SAT, evaporation (E), and P in Table 2 and Figs. 6a–c. These

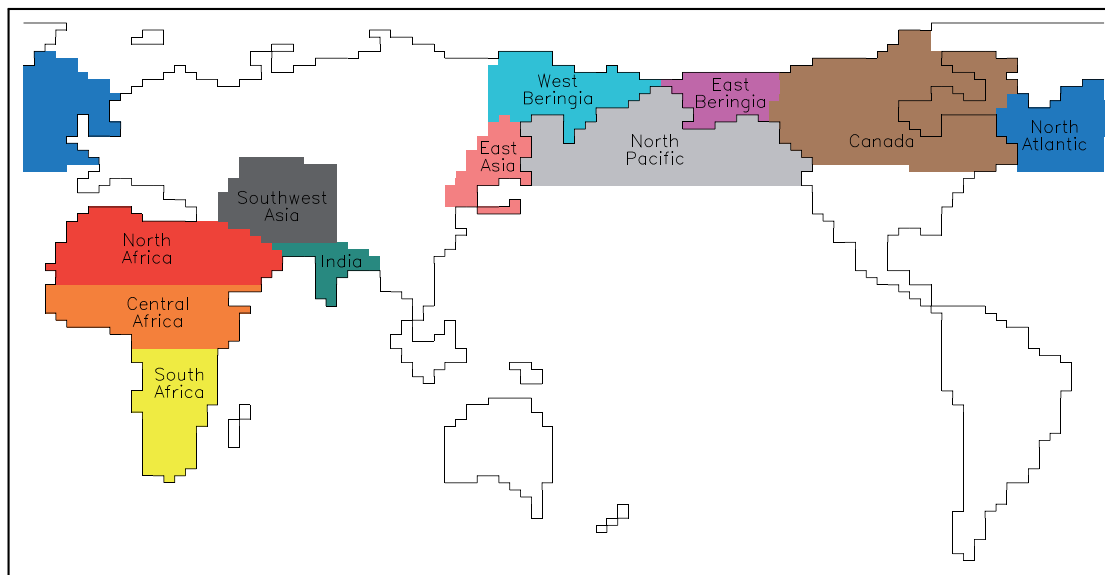


Fig. 3. Regions defined for the analysis of climate model simulations. The identification of regional impacts was based on model simulations pertaining to the regions relating to: (a) Beringia: East Asia, Western Beringia, Eastern Beringia, Canada, and the North Pacific, and (b) Africa: South Africa, Central, and North Africa, Southwest Asia, and India, as well as the North Atlantic Ocean. Black coastal outlines are drawn around land points specified in the model.

combined with Figs. 7a–e, which are graphic illustrations of regional average NPP of the five modelled vegetation types, make it evident that regional LGM climate anomalies can vary significantly from each other and from the respective global LGM climate anomalies.

5.2.1. East Asia and Beringia

Here we review the modeled climate of Beringia and surrounding regions, which are the focus of migration theories for the peopling of the Americas.

The LGM simulation indicates average SATs were reduced by 8 °C in Eastern Beringia and 7 °C in Western Beringia. These correlate reasonably well with estimates based on fossil beetle assemblages from Alaska by Elias (2001) that signify LGM temperatures during the warmest month in Southwest Alaska were about 4 °C colder than modern, in Yukon and Interior Alaska were up to 6.4 °C colder than modern, and in interior continental regions were 10–24 °C colder than today. LGM simulated average SATs for Western Beringia are cooler than estimates based on fossil beetle assemblages from northeast Siberia by Alfimov and Berman (2001), which imply mean July temperatures were 12–13 °C, essentially the same as modern. Interior fossil beetle localities appear to represent colder LGM localities than sites more proximal to Central Beringia. The LGM simulation for the North Pacific Ocean region provides some insights into the LGM conditions in Central Beringia and along the southern edge of the Beringian continental shelf. Modelled SATs in the North Pacific Ocean region were about 3 °C warmer than Eastern Beringia and about 2 °C warmer than Western Beringia in the North Pacific Ocean perhaps the result of a warming maritime influence.

The LGM model simulates a reduction in P in Western Beringia, which is consistent with recent interpretations of limited glacial ice coverage in Western Beringia (Svendsen et al., 1999; Brigham-Grette et al., 2004). LGM model simulation shows reduced P of 55 mm/yr in Western Beringia, which equates to P levels of 84% of PD (see Table 2). Eastern Beringia shows a greater reduction in P of 131 mm/a, which equates to P levels of 73% of PD, which is consistent with findings of Barber and Finney (2000) whereby Alaskan lake levels suggest precipitation was 40–75% less than modern. Our results do not support interpretations by Clague et al. (2004) that evaporation (E) exceeded P in most Eastern Beringia lake basins. However, it does suggest that E minus P increased in both Eastern Beringia and Western Beringia during the LGM relative to PD, suggesting that both regions were drier in the LGM than today. These findings are consistent with geomorphological interpretations by Glushkova (2001) of limited glaciation during the LGM in both Eastern and Western Beringia. The LGM simulation further shows higher P and lower E in Eastern Beringia than Western Beringia during the LGM, making Eastern Beringia wetter than Western Beringia, as is the case in the PD. The net impact of higher P and lower E, combined with a 1 °C greater reduction in SAT in Eastern Beringia compared with Western Beringia, appears to be larger expansion of barren soil coverage in Eastern Beringia than Western Beringia, although both regions show more than a 200% increase in modelled barren soil coverage in LGM relative to PD (Table 3). A large percentage reduction in average NPP and coverage of needleleaf trees is modelled for both Western and Eastern Beringia relative to PD; however a greater reduction occurs in Western Beringia. Fig. 5a shows in red, regions of

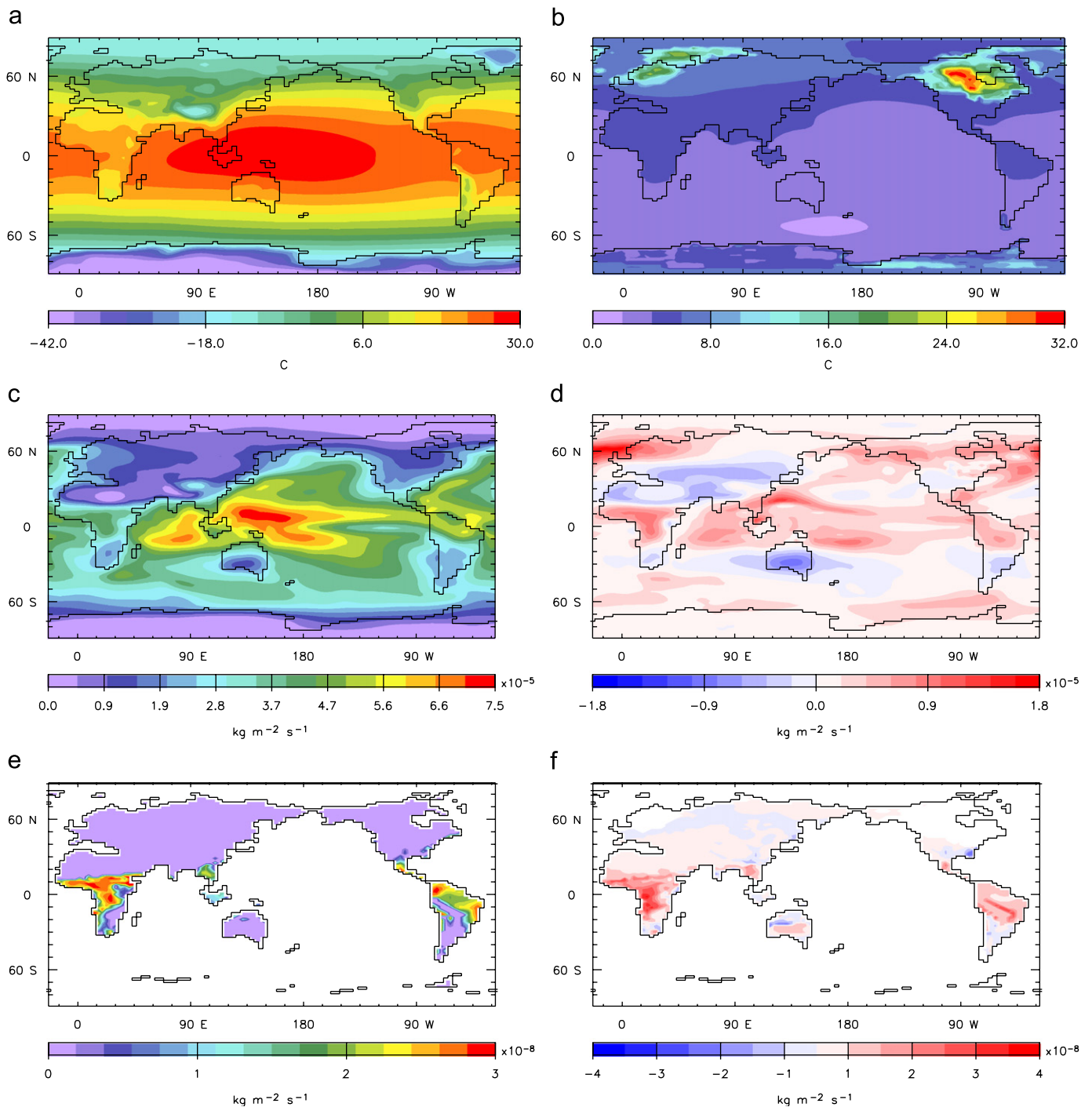


Fig. 4. Maps showing the present day (PD) model simulated values for surface air temperature (SAT), precipitation (P), and average net primary productivity (NPP) for broadleaf trees as well as the PD minus last glacial maximum (LGM) model simulated climate anomalies: (a) PD modelled SAT; (b) PD minus LGM modelled SAT. Colour scale refers to the amount PD SATs exceed LGM SATs in degrees centigrade; (c) PD modelled P. Present day modelled precipitation where regions in red receive the greatest annual precipitation, and areas in purple receive the least precipitation; (d) PD minus LGM modelled P. Colour scale refers to the amount PD precipitation exceeds LGM. Areas in red show reduced P in the LGM, areas in blue show increased P in the LGM; (e) PD modelled average NPP for broadleaf trees; and (f) PD minus LGM modelled average NPP difference for broadleaf trees. Colour scale refers to the amount PD broadleaf tree average NPP exceeds that of LGM. Areas in red show reduced LGM broadleaf average NPP, areas in blue show increased LGM broadleaf average NPP. *Note:* PD = model simulation at year 2000; LGM = 21 ka BP model simulation with ice extent and height specified according to Peltier's (2004) ICE-5G model; PD-LGM = present day model simulation minus LGM model simulation.

significant reduction in needleleaf coverage during the LGM relative to PD; this is particularly evident in Eastern and Western Beringia. These findings are consistent with

paleoenvironmental interpretations of virtually treeless conditions in Eastern Beringia during the LGM by Guthrie (1990, 2001) and Ritchie (1984) and others. In addition the

Table 1
Globally averaged precipitation and surface air temperature anomalies as well as globally averaged net primary productivity (NPP) and areal coverage (FRAC) for various vegetation types

Name of model output	Precipitation (mm/a)	Atmospheric surface temperature (°C)	NPP broadleaf trees (g/m ² /a)	FRAC broadleaf trees (%)	NPP needleleaf trees (g/m ² /a)	FRAC needleleaf trees (%)	NPP grass (g/m ² /a)	FRAC C3 grass (%)	NPP C4 grass (g/m ² /a)	FRAC C4 grass (%)	NPP shrubs (g/m ² /a)	FRAC shrubs (%)	FRAC barren soil (%)
PD (year 2000)	1079	14	174.2	19.8	101.6	19.9	157.5	31.2	47.7	6.3	39.1	9.2	13.5
LGM	1023	10	64.7	12.1	61.9	14.6	127.5	38.2	80.5	11.9	29	11.2	11.8
PD-LGM	56	4.4	132.2	10.4	24.9	1.6	24.0	-7.8	-25.9	-4.9	12	-2.1	2.9
LGM													

Note: PD = model simulation at year 2000; LGM = 21 ka BP model simulation ice extent and height specified according to Peltier's (2004) ICE-5G model; PD-LGM = present day model simulation minus LGM model simulation; due to differences in topography between PD and LGM, the differences between PD and LGM NPP and FRAC do not exactly coincide with numerical differences.

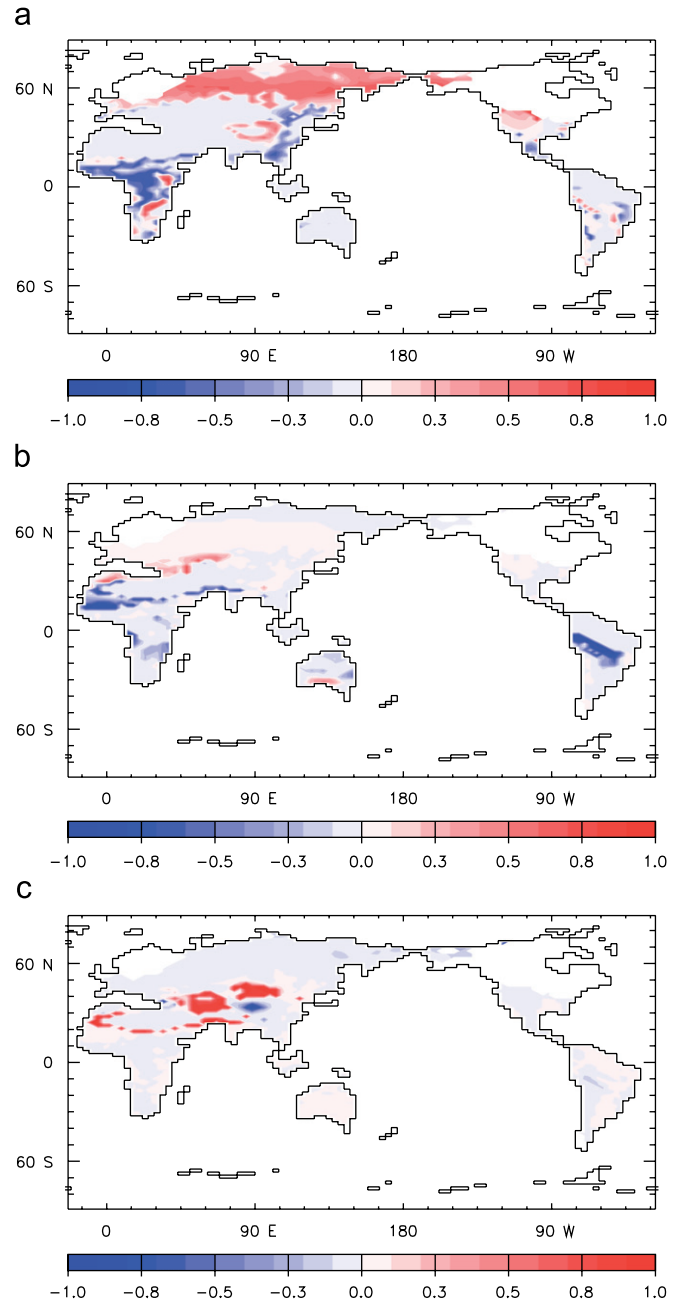


Fig. 5. Maps showing present day (PD) minus last glacial maximum (LGM) model simulated proportional coverage anomalies. Colour scales refer to the amount PD vegetation coverage exceeds that of the LGM. Areas shown in red indicate reduced LGM vegetation coverage; areas in blue indicate increased LGM vegetation coverage: (a) Needleleaf trees; (b) C4 grass; and (c) Barren soil. Note: PD = model simulation at year 2000; LGM = 21 ka BP model simulation with ice extent and height specified according to Peltier's (2004) ICE-5G model.

LGM model simulation suggests that although both regions were significantly less treed during the LGM than today, Eastern Beringia appears to have been slightly more heavily treed than Western Beringia. Reduced average NPP of shrubs modelled in both Eastern and Western Beringia during the LGM (Table 3) is consistent with LGM vegetation change interpretations by Bigelow et al. (2003)

Table 2
Difference in last glacial maximum (LGM) regional surface air temperature (SAT), evaporation (E), and precipitation (P) relative to present day (PD)

Region	LGM minus PD SAT (°C)	LGM minus PD E (mm/a)	LGM minus PD P (mm/a)
Global	−4	−56	−56
E. Asia	−6	20	51
E. Beringia	−8	−64	−131
W. Beringia	−7	−25	−55
Canada	−18	−170	−121
S. Africa	−4	−24	−59
C. Africa	−5	−93	−181
N. Africa	−5	58	59
SW Asia	−6	107	122
India	−5	26	23
N. Atlantic Ocean	−7	−366	−306
N. Pacific Ocean	−5	−119	−95

Refer to Fig. 3 for a definition of the regions.

Note: LGM = 21 kaBP model simulation with ice extent and height specified according to Peltier's (2004) ICE-5G model; PD = model simulation at year 2000.

and vegetation modelling by Kaplan (2001) and Kaplan et al. (2003), although shrub coverage reduction is not as extensive in our model simulations. Disparities may be the result of more restricted glacial ice coverage in East Siberia in our model simulations than that used by Kaplan. Our LGM simulation further indicates that C3 grass more than doubled its coverage in both Eastern and Western Beringia (Table 3). A grassland dominated environment in Eastern Beringia is consistent with late-Pleistocene macrofossil evidence from Yukon, Canada dominated by sage, bunchgrasses and grass-like plants considered by Zazula et al. (2003) to have flourished in cold, dry steppe conditions. However, although modelled C3 grass coverage was more than double PD in both regions, increased C3 grass productivity was limited to Western Beringia.

The LGM simulation also shows a reduction in E in the North Pacific Ocean that is slightly more than the reduction in P allowing for a small relative decrease in E minus P relative to PD, making the region slightly wetter than PD, a finding which is consistent with that postulated by Guthrie (2001) for Central Beringia. The LGM simulation also indicates that subaerial continental shelf regions exposed during the LGM were vegetated with C3 grass and shrubs. These findings support interpretations by Elias et al. (1996) of moderately dry to mesic environments interspersed with marshes and small ponds and by Yurtsev (2001) of shrub tundra covered lowlands on the Bering Land Bridge.

As indicated in Table 2, our simulations show increased P and E during the LGM in East Asia; the increase in P is more than twice that of E, making the region wetter than PD. The LGM simulation shows SAT decreases slightly

more in East Asia, by 6 °C, than the global average reduction of 4 °C. East Asia shows reduced broadleaf tree average NPP, reduced needleleaf average NPP, reduced C4 grass average NPP, slightly increased C3 grass average NPP, and a doubling of shrub average NPP in the LGM relative to PD (Table 3). These changes in average NPP are coincident with minor changes in needleleaf tree, C3 grass, and C4 grass coverage and a nearly 350% increase in shrub coverage relative to PD.

Our model LGM simulation shows higher average NPP for needleleaf trees and an increase in shrub average NPP in East Asia relative to Eastern and Western Beringia. C4 grass and broadleaf trees are only present in East Asia. Both East Asia and Western Beringia show an increase in C3 grass average NPP in LGM relative to PD (Table 3). These findings suggest that during the LGM, species living in Western Beringia that were dependant on needleleaf trees and shrub vegetation would have found better habitat conditions in East Asia. However, East Asian species dependant on broadleaf, needleleaf, and C4 grass habitats would have found their conditions worsening during the LGM. Alternatively species utilizing C3 grass, despite a marginally higher average NPP of C3 grass in East Asia relative to PD, would have found better conditions in Western Beringia where average NPP was also higher, but C3 grass coverage was expanding. Species previously inhabiting needleleaf tree, shrub, and to a lesser extent C3 habitats would be squeezed out of Eastern Beringia during the LGM. Those species moving out of East Asian broadleaf, needleleaf, and C4 grass environments, Eastern and Western Beringian needleleaf and shrub environments, and Eastern Beringian C3 grass habitat during the LGM may have found their way onto the subaerial continental shelf.

5.2.2. Africa, Southwest Asia, and India

The LGM simulation (Figs. 4d and 6b,c) lends some support to Hooghiemstra et al.'s (1992) interpretation of moister conditions northwest of the Sahara, in that the model indicates that both E and P increased in North Africa (Table 2) during the LGM relative to PD resulting in a very small increase in E minus P. This contrasts with Central Africa where both P and E decreased in the LGM although the reduction in P was nearly twice the reduction in E resulting in increased aridity (Table 2). South Africa experienced a reduction in E and P, but to a lesser extent than Central Africa. Lake Chad is located on the boundary between the modelled regions of North and Central Africa where our LGM simulation indicates increased aridity and C4 grass expansion confirming Maley's (1977) and Servant and Servant-Vildary's (1980) interpretations of persisting semi-desert grassland during the LGM.

The 5 °C reduction in modelled SAT for the LGM in North Africa (Table 2) equates with that observed in Central Africa (5 °C), whereas in South Africa SAT is reduced by 4 °C. These findings are consistent with estimations by Maley and Livingstone (1983), Maley

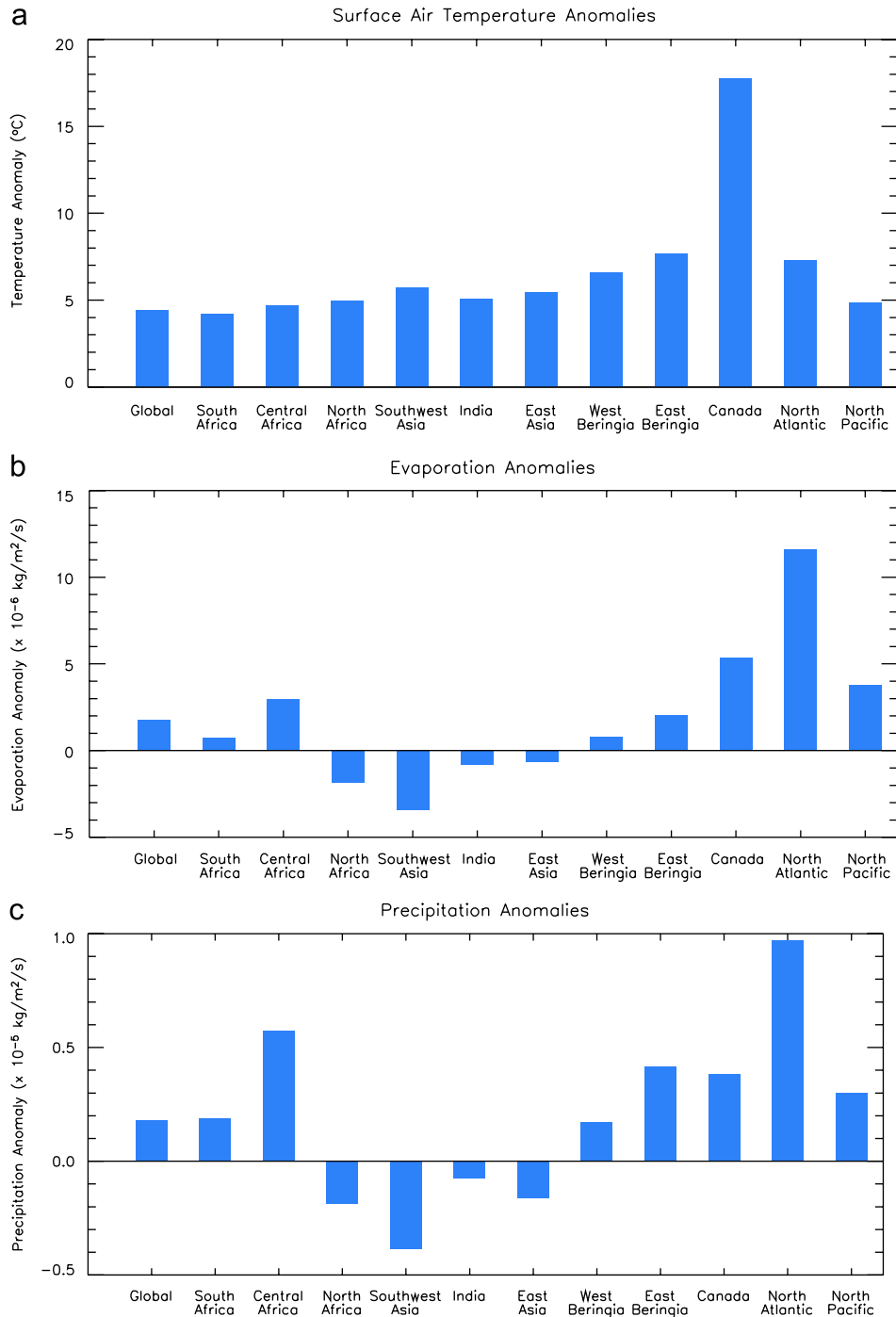


Fig. 6. Graphs showing global and regional surface air temperature (SAT), evaporation (E), and precipitation (P) anomalies for present day (PD) minus last glacial maximum (LGM) model simulations: (a) SAT anomalies; (b) E anomalies; and (c) P anomalies. Positive anomalies indicate levels higher in the PD than the LGM; negative anomalies indicate levels lower in the PD than the LGM. Note: PD = model simulation at year 2000; LGM = 21 ka BP model simulation ice extent and height specified according to Peltier's (2004) ICE-5G model.

(1981, 1989, 1991, 1996) and Livingstone (1993) of reductions in temperature between 3 and 8 °C and Maley (1989) and Livingstone (1993) between 5 and 6 °C cooler than at present in inter-tropical Africa during the LGM, and slightly warmer than the 5 °C reduction estimated by Deacon and Deacon (1999) from isotope records at Congo Cave, South Africa.

The LGM model shows a decrease in broadleaf tree coverage and NPP for North, Central and South Africa, although the greatest impact occurs in South Africa followed by Central Africa (Table 3 and Figs. 4e, f). Reductions in broadleaf coverage are met with expansions in needleleaf coverage in Central and North Africa (Fig. 5a). Central Africa experiences the largest expansions

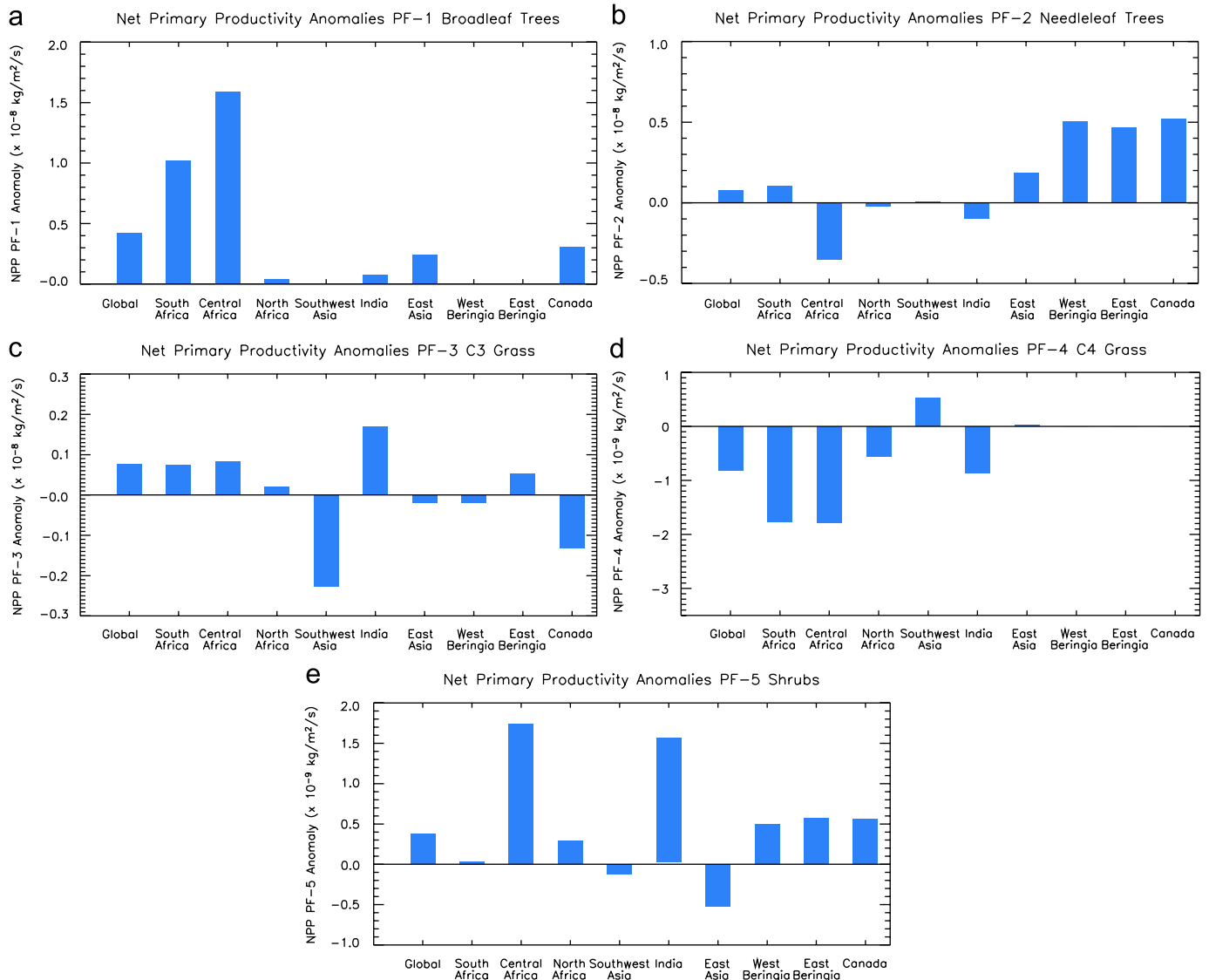


Fig. 7. Graphs showing average net primary productivity (NPP) anomalies for present day (PD) minus last glacial maximum (LGM) model simulations: (a) broadleaf trees; (b) needleleaf trees; (c) C3 grass; (d) C4 grass; and (e) shrubs. Positive anomalies indicate average NPP levels higher in the PD than the LGM; negative anomalies indicate average NPP levels lower in the PD than the LGM. *Note:* PD = model simulation at year 2000; LGM = 21 ka BP model simulation with ice extent and height specified according to Peltier's (2004) ICE-5G model.

in needleleaf tree coverage at 600% of PD, followed by North Africa at over 300% of PD. Areas shown in blue in Fig. 5a identify areas where needleleaf tree coverage is greater in the LGM simulation relative to PD; as apparent particularly in Central Africa. Needleleaf tree average NPP for the LGM is more than double PD in North Africa and more than triple PD in Central Africa (Table 3). Our LGM simulation shows large increases in C4 grass (Fig. 5b) and somewhat lesser increases in C3 grass coverage, particularly in Central and South Africa, and are consistent with findings by Deacon and Lancaster (1988) of an expanding semi-desert grassland in Central and South Africa and by Elenka et al. (2000) of a pervasive steppe consisting of a strong C4 grass component. C4 grass average NPP for the LGM is more than double PD in South Africa and Central Africa, with a slightly lesser increase in North Africa

(Table 3). Although the LGM simulation shows shrub coverage increases in South Africa, it decreases in Central and North Africa. Shrub average NPP is also reduced in the LGM simulation throughout Africa, with the greatest percentage change occurring in North Africa, followed by Central Africa (Table 3). Barren soil coverage increases by over five times in Central Africa, over two times in South Africa, but is reduced in North Africa, particularly in northwestern Africa (Table 3 and Fig. 5c).

These findings are consistent with interpretations of expanding desertification and increased aridity in Central and to a lesser extent South Africa during the LGM (Deacon and Lancaster, 1988; Thomas and Thorp, 1995; Johnson et al., 2002) and moister conditions in northwest Africa (Hooghiemstra et al., 1992). Vegetation coverage findings are consistent with interpretations of prevailing

Table 3

Regionally averaged percentage differences in last glacial maximum (LGM) average net primary productivity (NPP), and areal coverage (FRAC) for vegetation types during LGM relative to present day (PD)

Region	NPP broadleaf (%)	FRAC broadleaf (%)	NPP needleleaf (%)	FRAC needleleaf (%)	NPP C3 grass (%)	FRAC C3 grass (%)	NPP C4 grass (%)	FRAC C4 grass (%)	NPP shrubs (%)	FRAC shrubs (%)	FRAC soil (%)
Global	37	61	61	73	81	122	169	187	75	121	87
E. Asia	40	61	68	95	104	96	88	89	198	348	73
E. Beringia	–	–	6	8	88	216	–	–	45	63	288
W. Beringia	–	–	4	5	104	229	–	–	50	78	233
Canada	–	–	9	13	102	186	–	–	51	70	541
S. Africa	16	26	83	132	83	130	235	306	96	153	259
C. Africa	21	35	372	600	77	165	209	399	42	68	549
N. Africa	37	59	215	308	91	116	129	157	23	33	81
SW Asia	–	–	5	6	206	241	4	5	316	341	53
India	57	95	1815	2400	68	123	133	195	35	53	41
N. Atlantic Ocean	–	–	–	–	–	–	–	–	–	–	–
N. Pacific Ocean	–	–	–	–	–	–	–	–	–	–	–

Refer to Fig. 3 for a definition of the regions.

Note: LGM = 21 ka BP model simulation with ice extent and height specified according to Peltier's (2004) ICE-5G model; PD = model simulation at year 2000; NPP shown as a percentage of regional PD average NPP; FRAC shown as a percentage of regional PD FRAC.

vegetation of semi-deciduous forests and grasslands (Elenga et al., 1994; Maley and Brenac, 1998) and a large reduction in rainforest in West and Atlantic Equatorial Africa (Bengo and Maley, 1991; Lézine and Vergnaud-Grazzini, 1993; Jahns, 1996; Dupont et al., 1998; Jahns et al., 1998) during the LGM.

Contrary to LGM simulated vegetation anomalies for North and Central Africa, the adjacent region identified as Southwest Asia saw a doubling of C3 grass average NPP and a more than tripling of shrub average NPP and coverage at the expense of near elimination in needleleaf tree and C4 grass coverage and average NPP and a halving of barren ground coverage (Table 3). To the south in India, the LGM model simulation shows an expansion of needleleaf trees. However due to the small PD needleleaf coverage in India this increase is relatively minor, making LGM needleleaf coverage in India only slightly higher than North Africa and substantially lower than South and Central Africa. The LGM simulation also shows a near doubling in C4 grass coverage in India, combined with a reduction in shrub and broadleaf tree coverage and average NPP, and reduced barren soil coverage.

These findings suggest that during the LGM species utilizing C4 grass were experiencing a surplus environment in Africa, particularly Central and South Africa (Fig. 5b), whereas it is likely that those in Southwest Asia would have shifted to the consumption of C3 grass. Although C3 grass coverage was expanding across the region, C3 grass average NPP was reduced in all areas except Southwest Asia. Any species solely reliant on C3 grass habitat and unable to switch to utilization of C4 grass during the LGM, would have potentially migrated out of Africa and India and into Southwest Asia. Those species dependant on broadleaf trees in Africa and India during the LGM would

have seen their environment shrink (Fig. 4f) and its productivity reduced. Although Central Africa still provided the highest LGM broadleaf coverage in the region, species living in broadleaf tree habitats in North Africa and India would have experienced less initial strain from reduced coverage and average NPP. This strain would have increased in time if species from South and Central Africa moved into North Africa and India. Species inhabiting needleleaf tree habitats in Southwest Asia were likely squeezed out into adjacent India or more likely North and Central Africa, where these habitats were both productive and expanding. Alternatively, species dependant on shrub vegetation that found their habitat reduced in coverage and productivity in India, North Africa, and Central Africa would have found a more productive environment in Southwest Asia and to a lesser extent South Africa.

During the lowered sea level of the LGM much of the Agulhas bank off the coast of southeast Africa was exposed so that between Cape Agulhas and Plettenberg Bay the coastline lay 100 km or more south of the present-day position (Deacon and Deacon, 1999). The existence of this subaerial continental shelf and others like it surrounding Africa may have provided expanded productive habitats during the LGM, facilitating the survival and movement of species from one region to another. Faure et al. (2002) suggest that during glacial periods when sea level fell, hydrostatic changes resulted in the appearance of abundant fresh water on the subaerial continental shelves. As the interior of Africa became increasingly desiccated during the LGM, particularly in Central and South Africa, the emergent continental shelf would have provided an expanded, less arid, and more productive environment for terrestrial vegetation, animals, and humans displaced by

the changing climate of Africa. Further, development of productive habitats on the newly exposed shelf may assist in explaining contradictions in the African offshore pollen and lake-level evidence for the LGM (Goodfriend and Margaritz, 1988; Thomas and Thorp, 1995). Our findings suggest that although species dependant on C4 grasses throughout Africa and on needleleaf trees in North and Central Africa would have found their territory expanding and becoming increasingly productive during the LGM, those dependant on broadleaf trees across Africa, and shrubs in Central and North Africa would have been squeezed into a shrinking territory with reduced productivity. Those dependant on C3 grass would have seen the coverage of their habitat increasing, but productivity reduced, particularly in Central Africa, and may have shifted to consumption of C4 grass. Emergent shelves may have provided productive new territories to inhabit and links to other potentially habitable continental regions.

6. Conclusions

The Beringia region provides an example of a large contiguous northern hemisphere continental shelf that was subaerial and escaped large-scale glacial ice coverage during the LGM. It provided an expanded territory and a landbridge link between East Asia and North America where the influences of climate change were distinctly different and across which, some theories suggest, early people migrated when first peopling the Americas during or just subsequent to the LGM. Our LGM climate model simulation indicates cooler SATs in Eastern Beringia than either Western Beringia or Central Beringia, with SATs 8 °C colder than PD in Eastern Beringia, 7 °C colder in Western Beringia, and 5 °C colder in Central Beringia. The LGM simulation points out that although Central Beringia was wetter in the LGM than PD, and Eastern and Western Beringia were drier than PD, Eastern Beringia was relatively wetter than Western or Central Beringia during the LGM as is the case in the PD. These disparities may explain the slightly greater persistence of needleleaf trees in Eastern Beringia compared with Western Beringia and the increase in modelled C3 grass average NPP in Western Beringia relative to a reduction in Eastern Beringia.

The LGM simulation also indicates an increase in barren soil coverage in Eastern and Western Beringia. Substantial reductions in modelled average NPP of needleleaf trees and, to a lesser extent shrubs, in Eastern and Western Beringia implies that any species, including humans that were dependant on these environments, would have felt pressure to migrate elsewhere. As climate deteriorated towards the LGM, the newly exposed continental shelf provided an expanded environment available to support flora, fauna, and humans that had been displaced when their original territories became increasingly barren soil- or ice-covered, and/or reduced in productivity.

Our findings suggest that species dependant on C3 grass would have found an expanding C3 grass environment in Western Beringia and potentially Central Beringia, whereas those dependant on needleleaf tree habitat would have been squeezed out of Western and Eastern Beringia and may have migrated to East Asia where a diminishing needleleaf tree environment remained. The LGM model simulation shows increased P in East Asia and a slightly warmer SAT than Western Beringia. However, East Asia likely possessed a different needleleaf tree distribution than Beringia and was very distant from Eastern Beringia. Species reliant on shrub vegetation would have found an increasingly productive environment in East Asia and in the newly exposed habitat on the continental shelf. Movement from northern Canadian regions to areas south of the ice sheets would have been restricted when the Laurentide and Cordilleran ice sheets converged east of the Canadian Rocky Mountains during the LGM, further stimulating movement onto and habitation of the subaerial continental shelves of Canada.

The continental shelves of Africa and surrounding region may have provided productive refugia to species squeezed by shrinking and increasingly less productive habitats in Africa. Increased aridity and cooler temperatures resulted in an increase in coverage and average NPP of C4 grass habitats in Africa, particularly Central and South Africa. This came at the expense of broadleaf tree habitat across Africa, needleleaf tree habitat productivity in South Africa, C3 grass productivity across Africa, but especially in Central Africa, and shrub habitat in Central and particularly North Africa. Barren ground expanded in Central and South Africa. Reduced productivity and shifting vegetation of continental regions during the LGM may have squeezed flora, fauna, and human populations into the potentially more productive, freshwater spring fed (Faure et al., 2002), and proximally located newly exposed continental shelf.

LGC climate modelling combined with proxy records obtained from both the continental regions of Beringia, Africa and surrounding regions and their associated continental shelves will provide the best framework to ascertain the regional impacts of climate change. Understanding the influences of LGC climate, both on continental habitats and subaerial continental shelves during the LGC, is critical if we are to ascertain the feasibility of potential migration routes for early peoples as they expanded out of Africa and around the world.

Acknowledgements

The authors are grateful to funding from NSERC and CFCAS and to SSHRC for a fellowship for Renée Hetherington. The manuscript benefited from comments by Robert G.B. Reid and thoughtful reviews by Scott A. Elias and an anonymous reviewer. This paper is a contribution to Commission on Coastal and Marine Processes, INQUA—sub-aerially exposed continental

shelves since the Middle Pleistocene climatic transition and IGCP 464—Continental Shelves during the Last Glacial Cycle.

References

- Aguirre, E., Carbonell, E., 2001. Early human expansions into Eurasia: the Atapuerca evidence. *Quaternary International* 75, 11–18.
- Alfimov, A.V., Berman, D.I., 2001. Beringian climate during the Late Pleistocene and Holocene. *Quaternary Science Reviews* 20, 127–134.
- Anderson, P.M., Brubaker, L.B., 1994. Vegetation history of north central Alaska: a mapped summary of Late Quaternary pollen data. *Quaternary Science Reviews* 13, 71–92.
- Balter, M., 2002. What made humans modern? *Science* 295, 1219–1225.
- Barber, V.A., Finney, B.P., 2000. Late Quaternary paleoclimatic reconstructions for interior Alaska based on paleolake-level data and hydrologic models. *Journal of Paleolimnology* 24, 29–41.
- Barnosky, C.W., Anderson, P.M., Bartlein, P.J., 1987. Vegetational changes during the last deglaciation in the Pacific Northwest, Rocky Mountains, and Alaska. In: Ruddiman, W.F., Wright, Jr., H.E. (Eds.), *North America and Adjacent Oceans during the Last Deglaciation*. Geological Society of America, The Geology of North America v. K-3, Boulder, pp. 289–321.
- Bar-Yosef, O., 1994. The lower Paleolithic of the Near East. *Journal of World Prehistory* 8, 211–266.
- Behl, R.J., Kennett, J.P., 1996. Brief interstadial events in the Santa Barbara basin, NE Pacific, during the past 60 kyr. *Nature* 379, 243–246.
- Belmaker, M., Tchernov, E., Condemi, S., Bar-Yosef, O., 2002. New evidence for hominid presence in the Lower Pleistocene of the Southern Levant. *Journal of Human Evolution* 43, 43–56.
- Bengo, M.D., Maley, J., 1991. Analyses des flux polliniques sur la marge sud du Golfe de Guinée depuis 135 000 ans. *Comptes Rendus de l'Académie des Sciences-Earth and Planetary Science* 313, 843–849.
- Berger, A., 2001. The role of CO₂, sea level and vegetation during the Milankovitch-forced glacial–interglacial cycles. In: Bengtsson, O., Hammer, C.U. (Eds.), *Geosphere–Biosphere Interactions and Climate*. Cambridge University Press, New York.
- Bigelow, N.H., Brubaker, L.B., Edwards, M.E., Harrison, S.P., Prentice, I.C., Anderson, P.M., Andreev, A.A., Bartlein, P.J., Christiansen, T.R., Cramer, W., Kaplan, J.O., Lozhkin, A.V., Matveyeva, N.V., Murray, D.F., McGuire, A.D., Razzhivin, V.Y., Ritchie, J.C., Smith, B., Walker, D.A., Gajewski, K., Wolf, V., Holmqvist, B.H., Igarashi, Y., Kremenetski, K., Paus, A., Pisaric, M.F.J., Volkova, V.S., 2003. Climate change and Arctic ecosystems: 1. Vegetation changes north of 55° N between the last glacial maximum, mid-Holocene, and present. *Journal of Geophysical Research* 108 (D19), 8170.
- Bonan, G.B., Pollard, D., Thompson, S.L., 1992. Effects of boreal forest vegetation on global climate. *Nature* 359, 716–718.
- Bond, G., Showers, W., Chezebiet, M., Lotti, R., Almasi, P., deMenocal, P., Priore, P., Cullen, H., Hajdas, I., Bonani, G., 1997. A pervasive millennial-scale cycle in North Atlantic Holocene and glacial climates. *Science* 278, 1257–1266.
- Braconnot, P., Joussaume, S., Marti, O., Noblet, N., 1999. Synergistic feedbacks from ocean and vegetation on the African monsoon response to mid-Holocene insolation. *Geophysical Research Letters* 26, 2481–2484.
- Bräuer, G., 1989. The evolution of modern humans: a comparison of the African and non-African evidence. In: Mellars, P., Stringer, C. (Eds.), *The Human Revolution: Behavioural and Biological Perspectives on the Origins of Modern Humans*. Princeton University Press, Princeton, NJ, pp. 123–154.
- Brigham-Grette, J., Lozhkin, A.V., Anderson, P.M., Glushkova, O.Y., 2004. Paleoenvironmental conditions in Western Beringia before and during the last glacial maximum. In: Madsen, D.B. (Ed.), *Entering America: Northeast Asia and Beringia before the Last Glacial Maximum*. University of Utah Press, Salt Lake City, pp. 63–94.
- Brook, G.A., Haberyan, K.A., De Filippis, S., 1987. Evidence of a shallow lake at Tsodilo Hills, Botswana, 17,500 to 15,000 yr BP: further confirmation of a widespread Late Pleistocene humid period in the Kalahari Desert. *Palaeoecology of Africa* 23, 165–175.
- Brun, A., 1991. Reflexions sur les pluviaux et arides au Pleistocene superieur et a l' Holocene en Tunisie. *Palaeoecology of Africa* 22, 157–170.
- Clague, J.J., Mathewes, R.W., Ager, T.A., 2004. Environments of northwestern North America before the last glacial maximum. In: Madsen, D.B. (Ed.), *Entering America: Northeast Asia and Beringia before the Last Glacial Maximum*. University of Utah Press, Salt Lake City, pp. 29–61.
- Crowley, T.J., 1992. North Atlantic deep water cools the Southern Hemisphere. *Paleoceanography* 7, 489–497.
- Cutler, K.B., Edwards, R.L., Taylor, F.W., Cheng, H., Adkins, J., Gallup, C.D., Cutler, P.M., Burr, G.S., Bloom, A.L., 2003. Rapid sea-level fall and deep-ocean temperature change since the last interglacial period. *Earth and Planetary Science Letters* 206, 253–271.
- Dansgaard, W., Johnsen, S.J., Clausen, B., Dahl-Jensen, D., Gundestrup, N., Hammer, C.U., Oeschger, H., 1984. North Atlantic climatic oscillations revealed by deep Greenland ice. In: Hansen, J.E., Takahashi, T. (Eds.), *Climate Processes and Climate Sensitivity*. Geophysical Monograph 29. American Geophysical Union, Washington, DC, pp. 288–298.
- Dansgaard, W., White, J.W.C., Johnsen, S.J., 1989. The abrupt termination of the Younger Dryas climate event. *Nature* 339, 532–534.
- Dansgaard, W., Johnsen, S.J., Clausen, H.B., Dahl-Jensen, D., Gundestrup, N.S., Hammer, C.U., Hvidberg, C.S., Steffensen, J.P., Sveinbjörnsdóttir, J.E., Jouzel, J., Bond, G., 1993. Evidence for general instability of past climate from a 250 kyr ice core. *Nature* 364, 218–219.
- Deacon, J., 1990. Changes in the archaeological record in South Africa at 18000 BP. In: Soffer, O., Gamble, C. (Eds.), *The World at 18000 BP*. Unwin Hyman, London, pp. 170–188.
- Deacon, H.J., Deacon, J., 1999. Environments of the past. In: Deacon, H.J., Deacon, J. (Eds.), *Human Beginnings in South Africa*. David Philip Publishers, Cape Town, pp. 9–29.
- Deacon, J., Lancaster, N., 1988. *Late Quaternary Environments of Southern Africa*. Clarendon Press, Oxford.
- de Castro, J.M.B., Martínón-Torres, M., Carbonell, E., Sarmiento, S., Rosas, A., van der Made, J., Lozano, M., 2004. The Atapuerca sites and their contribution to the knowledge of human evolution in Europe. *Evolutionary Anthropology* 13, 25–41.
- Duarte, C., Mauricio, J., Pettitt, P.B., Souto, P., Trinkaus, E., van der Plicht, H., Zilhao, J., 1999. The early Upper Paleolithic human skeleton from the Abrigo do Lagar Velho (Portugal) and modern human emergence in Iberia. *Proceedings of the National Academy of Sciences of the United States of America* 96, 7604–7609.
- Dupont, L.D., 1993. Vegetation zones in North Western Africa during the Brunhes chron reconstructed from marine palynological data. *Quaternary Science Reviews* 12, 189–202.
- Dupont, L.M., Hooghiemstra, H., 1989. The Sahara–Sahelian boundary during the Brunhes chron. *Acta Botanica Neerlandica* 38, 405–415.
- Dupont, L., Marret, F., Winn, K., 1998. Land-sea correlation by means of terrestrial and marine palynomorphs from the equatorial East Atlantic: phasing of south-east trade wind and the oceanic productivity. *Palaeogeography, Palaeoclimatology, Palaeoecology* 155, 95–122.
- Ehlers, J., Gibbard, P.L., 2004a. *Quaternary Glaciations—Extent and Chronology, Part I: Europe*. Elsevier, Amsterdam, 475pp.
- Ehlers, J., Gibbard, P.L., 2004b. *Quaternary Glaciations—Extent and Chronology, Part II: North America*. Elsevier, Amsterdam, 440pp.
- Ehlers, J., Gibbard, P.L., 2004c. *Quaternary Glaciations—Extent and Chronology, Part III: South America, Asia, Africa, Australia, Antarctica*. Elsevier, Amsterdam, 380pp.
- Elena, H., Schwartz, D., Vincens, A., 1994. Pollen evidence of Late Quaternary vegetation and inferred climate changes in Congo. *Palaeogeography, Palaeoclimatology, Palaeoecology* 109, 345–356.
- Elena, H., Peyron, O., Bonnefille, R., Jolly, D., Cheddadi, R., Guiot, J., Andrieu, V., Bottema, S., Buchet, G., de Beaulieu, J.-L., Hamilton, A.C.,

- Maley, J., Marchant, R., Perez-Obiol, R., Reille, M., Riollet, G., Scott, L., Straka, H., Taylor, D., Van Campo, E., Vincens, A., Laarif, F., Jonson, H., 2000. Pollen-based biome reconstruction for southern Europe and Africa 18,000 yr BP. *Journal of Biogeography* 27, 621–634.
- Elias, S.A., 2001. Mutual climatic range reconstructions of seasonal temperatures based on late Pleistocene fossil beetle assemblages in Eastern Beringia. *Quaternary Science Reviews* 20, 77–92.
- Elias, S.A., Short, S.K., Phillips, R.L., 1996. The life and times of the Bering Land Bridge. *Nature* 382, 60–63.
- Elias, S.A., Short, S.K., Birks, H.H., 1997. Late Wisconsin environments of the Bering Land Bridge. *Palaeogeography, Palaeoclimatology, Palaeoecology* 136, 293–308.
- Endicott, P., López, J.C., Gonzalez, S., Cooper, A., 2004. Human mtDNA and the origins of the first Americans: what can archaeological specimens add? In: *Proceedings of the Second Symposium El Hombre Temprano en América*, Mexico City, Mexico, 6–10 September, 2004.
- Erlandson, J.M., 2002. Anatomically modern humans, maritime voyaging, and the Pleistocene colonization of the Americas. In: Jablonski, N.G. (Ed.), *The First Americans, The Pleistocene Colonization of the New World*. California Academy of Sciences, San Francisco, pp. 59–92.
- Ewen, T., Weaver, A.J., Schmittner, A., 2003. Modelling carbon cycle feedbacks during abrupt climate change. *Quaternary Science Reviews* 23, 431–448.
- Fairbanks, R.G., 1989. A 17,000-year glacio-eustatic sea level record: influence of glacial melting rates on the Younger Dryas event and deep-ocean circulation. *Nature* 342, 637–642.
- Farrera, I., Harrison, S.P., Prentice, I.C., Ramstein, G., Guiot, J., Bartlein, P.J., Bonnefille, R., Bush, M., Cramer, W., von Grafenstein, U., Holmgren, K., Hooghiemstra, H., Hope, G., Jolly, D., Lauritzen, S.-E., Ono, Y., Pinot, S., Stute, M., Yu, G., 1999. Tropical climates at the last glacial maximum: a new synthesis of terrestrial palaeoclimate data. I. Vegetation, lake-levels and geochemistry. *Climate Dynamics* 15, 823–856.
- Faure, H., Walter, R.C., Grant, D.R., 2002. The coastal oasis: ice age springs on emerged continental shelves. *Global and Planetary Change* 33, 47–56.
- Foley, J.A., Kutzbach, J.E., Coe, M.T., Levis, S., 1994. Feedbacks between climate and boreal forests during the Holocene epoch. *Nature* 371, 52–54.
- Gabunia, L., Vekua, A., Lordkipanidze, D., Swisher III, C.C., Ferring, R., Justus, A., Nioradze, M., Tvalchrelidze, M., Antón, S.C., Bosinski, G., Jöris, O., -de Lumley, M.-A., Majsuradze, G., Mouskhelishvili, A., 2000. Earliest Pleistocene hominid cranial remains from Dmanisi, Republic of Georgia: taxonomy, geological setting, and age. *Science* 288, 1019–1025.
- Gabunia, L., Antón, S.C., Lordkipanidze, D., Vekua, A., Justus, A., Swisher III, C.C., 2001. Dmanisi and dispersal. *Evolutionary Anthropology* 10, 158–170.
- Ganopolski, A., Kubatzki, C., Claussen, M., Brovkin, V., Petoukhov, V., 1998. The influence of vegetation–atmosphere–ocean interaction on climate during the mid-Holocene. *Science* 280, 1916–1919.
- Giresse, P., Le Ribault, M., 1990. Reconstitution palaeogeographique des derniers épisodes du Quaternaire littoral du Congo par L'Etude exoscopique des Quartz. In: Lanfranchi, R., Schwartz, D. (Eds.), *Paysages quaternaires de L'Afrique Centrale Atlantique*. ORSTOM, collection Didactiques, Paris, pp. 98–99.
- Glushkova, O.Y., 2001. Geomorphological correlation of Late Pleistocene glacial complexes of Western and Eastern Beringia. *Quaternary Science Reviews* 20, 405–417.
- González-José, R., González-Martin, A., Hernández, M., Pucciarelli, H.M., Sardi, M., Rosales, A., Van der Molen, S., 2003. Craniometric evidence for Palaeoamerican survival in Baja California. *Nature* 425, 62–65.
- Goodfriend, G.A., Margaritz, M., 1988. Palaeosols and late Pleistocene rainfall fluctuations in the Negev Desert. *Nature* 332, 144–147.
- Grosswald, M.G., 1988. An Antarctic-style ice sheet in the Northern Hemisphere: towards new global glacial theory. *Polar Geography and Geology* 12, 239–267.
- Grosswald, M.G., 1998. Late Weichselian ice sheets in Arctic and Pacific Siberia. *Quaternary International* 45–46, 3–18.
- Grosswald, M.G., Hughes, T.J., 1995. Paleoglaciology's grand unsolved problem. *Journal of Glaciology* 41, 313–322.
- Grosswald, M.G., Hughes, T.J., 2002. The Russian component of an Arctic ice sheet during the last glacial maximum. *Quaternary Science Reviews* 21, 121–146.
- Guthrie, R.D., 1990. *Frozen Fauna of the Mammoth Steppe*. University of Chicago Press, Chicago, 338pp.
- Guthrie, R.D., 2001. Origin and causes of the mammoth steppe: a story of cloud cover, woolly mammal tooth pits, buckles, and inside-out Beringia. *Quaternary Science Reviews* 20, 549–574.
- Hamilton, T.D., Ashley, G.M., Reed, K.M., Schweger, C.E., 1993. Late Pleistocene vertebrates and other fossils from Epiguruk, northwestern Alaska. *Quaternary Research* 39, 381–389.
- Hetherington, R., Barrie, J.V., 2004. Interaction between local tectonics and glacial unloading on the Pacific margin of Canada. *Quaternary International* 120, 65–77.
- Hetherington, R., Barrie, J.V., Reid, R.G.B., MacLeod, R., Smith, D.J., James, T.S., Kung, R., 2003. Late Pleistocene coastal paleogeography of the Queen Charlotte Islands, British Columbia, Canada, and its implications for terrestrial biogeography and early postglacial human occupation. *Canadian Journal of Earth Sciences* 40, 1755–1766.
- Hetherington, R., Barrie, J.V., Reid, R.G.B., MacLeod, R., Smith, D.J., 2004. Paleogeography, glacially induced crustal displacement, and Late Quaternary coastlines on the continental shelf of British Columbia, Canada. *Quaternary Science Reviews* 23, 295–318.
- Hoelzmann, P., Gasse, F., Dupont, L.M., Salzmann, M., Staubwasser, M., Leuschner, D.C., Sirocko, F., 2004. Palaeoenvironmental changes in the arid and sub-arid belt (Sahara–Sahel–Arabian Peninsula) from 150 kyr to present. In: Battarbee, R.W., Gasse, F., Stickley, C.E. (Eds.), *Past Climate Variability through Europe and Africa, Series: Developments in Palaeoenvironmental Research*, vol. 6. Springer Publishers, Netherlands, pp. 219–256.
- Holden, C., 1999. Archaeology: were Spaniards among the first Americans? *Science* 286, 1467–1468.
- Hooghiemstra, H., Stalling, H., Agwu, C.O.C., Dupont, L.M., 1992. Vegetational and climatic changes at the northern fringe of the Sahara 250,000–5000 years BP. *Review of Palaeobotany and Palynology* 74, 1–53.
- Hopkins, D.M., Matthews, Jr., J.V., Schweger, C.E., Young, S.B. (Eds.), 1982. *Paleoecology of Beringia*. Academic Press, New York, 489pp.
- Hublin, J.-J., 2000. Modern–nonmodern hominid interactions: a Mediterranean perspective. In: Bar-Yosef, O., Pilbeam, D. (Eds.), *Geography of Neandertals and Modern Humans in Europe and the Greater Mediterranean*. Peabody Museum of Archaeology and Ethnology, Cambridge, MA, pp. 157–182.
- IGCP Project 464, 2001–2006. International Geological Correlation Program, Project 464, Continental Shelves during the Last Glaciation: Knowledge and Applications. <<http://tetide.geo.uniroma1.it/IGCP464/>>.
- Imbrie, J., Hays, J.D., Martinson, D.G., McIntyre, A., Mix, A.C., Morley, J.J., Pisias, N.G., Prell, W.L., Shackleton, N.J., 1984. The orbital theory of Pleistocene climate: support from a revised chronology of the marine $\delta^{18}\text{O}$ record. In: Berger, A.L., Hays, J., Kukla, G., Salzman, B. (Eds.), *Milankovitch and Climate, Part 1*. D. Reidel, Dordrecht, pp. 269–305.
- Jahns, S., 1996. Vegetation history and climatic changes in west equatorial Africa during the late Pleistocene and the Holocene based on a marine pollen diagram from the Congo fan. *Vegetational History and Archaeobotany* 5, 207–213.
- Jahns, S., Hüls, M., Sarnthein, M., 1998. Vegetation and climate history of west equatorial Africa based on a marine pollen record off Liberia (site GIK 16776) covering the last 400,000 years. *Review of Palaeobotany and Palynology* 102, 277–288.
- Jansen, J.H.F., 1990. Glacial–interglacial oceanography of the south-eastern Atlantic Ocean and the palaeoclimate of west-central Africa. In: Lanfranchi, R., Schwartz, D. (Eds.), *Paysages Quaternaires de*

- L'Afrique Centrale Atlantique. Editions de l'Orstom, Paris, pp. 110–123.
- Johnson, T.C., Brown, E.T., McManus, J., Barry, S., Barker, P., Gasse, F., 2002. A high-resolution paleoclimate record spanning the past 25,000 years in southern East Africa. *Science* 296, 113–132.
- Jolly, D., Prentice, C.I., Bonnefille, R., Ballouche, A., Bengo, M., Brenac, P., Buchet, G., Burney, D., Cazet, J.-P., Cheddadi, R., Ederh, T., Elenga, H., Elmoutaki, S., Guiot, J., Laarif, F., Lamb, H., Lezine, A.-M., Maley, J., Mbenza, M., Peryon, O., Reille, M., Reynaud-Farrera, I., Riollet, G., Ritchie, J.C., Roche, E., Scott, L., Ssemmanda, I., Straka, H., Umer, M., Van Camp, E., Vilimballo, S., Vincens, A., Waller, M., 1998. Biome reconstruction from pollen and plant macrofossil data for Africa and the Arabian peninsula at 0 and 6000 years. *Journal of Biogeography* 25, 1007–1027.
- Justino, F., 2004. The influence of boundary conditions on the last glacial maximum: Climate Dynamics. Shaker Verlag, Aachen.
- Kaplan, J.O., 2001. Geophysical applications of vegetation modeling. Ph.D. Thesis, Lund University, Lund, Sweden, 114pp.
- Kaplan, J.O., Bigelow, N.H., Prentice, I.C., Harrison, S.P., Bartlein, P.J., Christensen, T.R., Cramer, W., Matveyeva, N.V., McGuire, A.D., Murray, D.F., Razzhivin, V.Y., Smith, B., Walker, D.A., Anderson, P.M., Andreev, A.A., Brubaker, L.B., Edwards, M.E., Lozhkin, A.V., 2003. Climate change and Arctic ecosystems: 2. Modeling, paleodata-model comparisons, and future projections. *Journal of Geophysical Research* 108 (D19), 8171.
- Kennett, J.P., Ingram, B.L., 1995. A 20,000 year record of ocean circulation and climate change from the Santa Barbara basin. *Nature* 377, 510–514.
- Kotilainen, A.T., Shackleton, N.J., 1995. Rapid climate variability in the North Pacific Ocean during the past 95,000 years. *Nature* 377, 323–326.
- Ku, T.-L., Kimmel, M.A., Easton, W.H., O'Neil, T.J., 1974. Eustatic sea level 120,000 years ago on Oahu, Hawaii. *Science* 183, 959–962.
- Lambeck, K., Esat, T.M., Potter, E.-K., 2002. Links between climate and sea levels for the past three million years. *Nature* 419, 199–206.
- Lang, C., Leuenberger, M., Schwander, J., Johnsen, J., 1999. 16 °C rapid temperature variation in central Greenland 70,000 years ago. *Science* 286, 934–937.
- Langbroek, M., Roebroeks, W., 2000. Extraterrestrial evidence on the age of the hominids from Java. *Journal of Human Evolution* 38, 595–600.
- Larick, R., Ciochon, R.L., Zaim, Y., Sudijono, Suminto, Rizal, Y., Aziz, F., Reagan, M., Heizler, M., 2001. Early Pleistocene ⁴⁰Ar/³⁹Ar ages for Bapang Formation hominins, Central Java, Indonesia. *Proceedings of the National Academy of Sciences of the United States of America* 98, 4866–4871.
- Lézine, A.M., 1991. West African paleoclimates during the last climatic cycle inferred from an Atlantic Deep-Sea Pollen record. *Quaternary Research* 35, 456–463.
- Lézine, A.M., Vergnaud-Grazzini, C., 1993. Evidence of forest extension in West Africa since 22,000 BP: a pollen record from eastern tropical Atlantic. *Quaternary Science Reviews* 12, 203–210.
- Livingstone, D.A., 1993. Evolution of African climate. In: Goldblatt, P. (Ed.), *Biological Relationships between Africa and South America*. Yale University, Connecticut, pp. 455–499.
- Lowell, T.V., Heusser, C.J., Andersen, B.G., Moreno, P.I., Hauser, A., Denton, G.H., Heusser, L.E., Schluchter, C., Marchant, D.R., 1995. Interhemispheric symmetry of paleoclimatic events during the last glaciation. *Science* 269, 1541–1549.
- Mackey, K.G., Fujita, K., Gunbina, L.V., Kovalev, V.N., Imaev, V.S., Koz'min, B.M., Imaeva, L.P., 1997. Seismicity of the Bering Strait region: evidence for a Bering block. *Geology* 25, 979–982.
- Maley, J., 1977. Palaeoclimates of central Sahara during the early Holocene. *Nature* 269, 573–577.
- Maley, J., 1981. Palynologic studies in the basin of Chad and paleoclimatology of 30,000 years north-tropical Africa at the time current. *Work and Documents ORSTOM* 129, p. 586.
- Maley, J., 1989. Late Quaternary Changes in the African rainforest. In: Leinen, M., Sarnthein, M. (Eds.), *Palaeoclimatology and Palaeome-teology; Modern and Past Patterns of Global Transport*. Kluwer Academic Publishers, Dordrecht, pp. 585–616.
- Maley, J., 1991. African rainforest vegetation and palaeoenvironments during the late Quaternary. *Climate Change* 19, 79–98.
- Maley, J., 1996. The African rainforest: Main characteristics of changes in vegetation and climate from the Upper-Cretaceous to the Quaternary. In: Alexander, J., Swaine, M.D., Watling, R. (Eds.), *Essays on the Ecology of the Congo-Guinean rainforest*. *Proceedings of the Royal Society of London Series B-Biological Sciences* 104, 31–73.
- Maley, J., Brenac, P., 1998. Vegetation dynamics, palaeoenvironments and climatic changes in the forest of Western Cameroon during the last 28,000 years BP. *Review of Palaeobotany and Palynology* 99, 157–178.
- Maley, J., Livingstone, D.A., 1983. Extension d'un element montagnard dans le sud du Ghana au Pleistocene Superieur et à l'Holocene Inferieur: premières données polliniques. *Comptes Rendus de l'Académie des Sciences-Earth and Planetary Science* 196, 1287–1292.
- Manley, W.F., 2002. Post-glacial Flooding of the Bering Land Bridge: A Geospatial Animation, vol. 1. INSTAAR, University of Colorado, <http://instaar.colorado.edu/QGISL/bering_land_bridge>.
- Matthews, H.D., Weaver, A.J., Eby, M., Meissner, K.J., 2003a. Radiative forcing of climate by historical land cover change. *Geophysical Research Letters* 30 (2), 27:1–27:4, 1055.
- Matthews, H.D., Weaver, A.J., Meissner, K.J., Gillett, N.P., Eby, M., 2003b. Natural and anthropogenic climate change: Incorporating historical land cover change, vegetation dynamics and the global carbon cycle. *Climate Dynamics* 22, 461–479.
- McBrearty, S., Brooks, A.S., 2000. The revolution that wasn't: a new interpretation of the origin of modern human behaviour. *Journal of Human Evolution* 39, 453–563.
- Meissner, K.J., Weaver, A.J., Matthews, H.D., Cox, P.M., 2003. The role of land-surface dynamics in glacial inception: a study with the UVic Earth System Model. *Climate Dynamics* 21, 515–537.
- Neves, W.A., Powell, J.F., Ozolins, E.G., 1999. Extra-continental morphological affinities of Lapa Vermelha IV, Hominid 1: a multivariate analysis with progressive numbers of variables. *Homo* 50, 263–282.
- O'Connell, J.F., Allen, J., 2004. Dating the colonization of Sahul (Pleistocene Australia-New Guinea): a review of recent research. *Journal of Archaeological Science* 31, 835–853.
- Oeschger, H., Beer, J., Siegenthaler, U., Stauffer, B., Dansgaard, W., Langway, C.C., 1984. Late glacial climate history from ice cores. In: Hansen, J.E., Takahashi, T. (Eds.), *Climate Processes and Climate Sensitivity*. *Geophysical Monographs* 29. American Geophysical Union, Washington, DC, pp. 299–306.
- Partridge, T.C., Scott, L., Hamilton, J.E., 1999. Synthetic reconstructions of southern African environments during the last glacial maximum (21–18 kyr) and the Holocene Altithermal (8–6 kyr). *Quaternary International* 57–58, 207–214.
- Peltier, W.R., 2004. Global glacial isostasy and the surface of the ice-age Earth: the ICE-5G (VM2) model and GRACE. *Annual Review of Earth and Planetary Sciences* 31, 111–149.
- Petit, J.R., Jouzel, J., Raynaud, D., Barkov, N.I., Barnola, J.-M., Basile, I., Bender, M., Chappellaz, J., Davis, M., Delayque, G., Delmotte, M., Kotlyakov, V.M., Legrand, M., Lipenkov, V.Y., Lorius, C., Pépin, L., Ritz, C., Saltzman, E., Stevenard, M., 1999. Climate and atmospheric history of the past 420,000 years from the Vostok ice core, Antarctica. *Nature* 399, 429–436.
- Ritchie, J.C., 1984. *Past and Present Vegetation of the Far Northwest of Canada*. University of Toronto Press, Toronto, 251pp.
- Roberts, R.G., Jones, R., Smith, M.A., 1990. Thermoluminescence dating of a 50,000-year-old human occupation site in northern Australia. *Nature* 345, 153–156.
- Roberts, R., Jones, R., Smith, M., 1994. Beyond the radiocarbon barrier in Australia. *Antiquity* 68, 611–616.
- Rossignol-Strick, M., Duzer, D., 1979. Late Quaternary pollen dinoflagellate cysts in marine cores off West Africa. "Meteor" Forschungs-Ergebnisse 30, 1–14.

- Salzmann, U., Hoelzmann, P., Morczinek, I., 2002. Late Quaternary climate and vegetation of the Sudanian zone of Northeast Nigeria. *Quaternary Research* 58, 73–83.
- Schmittner, A., Meissner, K.J., Eby, M., Weaver, A.J., 2002. Forcing of the deep ocean circulation in simulations of the last glacial maximum. *Paleoceanography* 17, 1015.
- Schmittner, A., Saenko, O.A., Weaver, A.J., 2003. Coupling of the hemispheres in observations and simulations of glacial climate change. *Quaternary Science Reviews* 22, 659–671.
- Schulz, H., von Rad, U., Erlenkeuser, H., 1998. Correlation between Arabian Sea and Greenland climate oscillations of the past 111,000 years. *Nature* 393, 54–57.
- Schulz, M., Timmermann, A., Paul, A., 2002. On the 1470-year pacing of Dansgaard–Oeschger warm events. *Paleoceanography* 17, 10.1029/2000PA000571.
- Sémah, F., Saleki, H., Falguères, C., 2000. Did early man reach Java during the Late Pliocene? *Journal of Archaeological Science* 27, 763–769.
- Servant, M., Servant-Vildary, S., 1980. L'environnement quaternaire du bassin du Tchad. In: Williams, M.A.J., Faure, H. (Eds.), *The Sahara and the Nile: Quaternary Environments and Prehistoric Occupation in Northern Africa*. A.A. Balkema, Rotterdam, pp. 133–163.
- Siegert, M.J., Marsiat, I., 2000. Numerical reconstructions of LGM climate across the Eurasian Arctic. *Quaternary Science Reviews* 20, 1595–1606.
- Siegert, M.J., Dowdeswell, J.A., Hald, M., Svendsen, J., 2001. Modelling the Eurasian Ice Sheet through a full (Weichselian) glacial cycle. *Global and Planetary Change* 31, 367–385.
- Stocker, T.F., 1998. The seesaw effect. *Science* 282, 61–62.
- Stokes, S., Thomas, D.S.G., Washington, R., 1997. Multiple episodes of aridity in southern Africa since the last interglacial. *Nature* 388, 154–158.
- Stringer, C.B., 1989. The origin of early modern humans: a comparison of the European and non-European evidence. In: Mellars, P., Stringer, C. (Eds.), *The Human Revolution: Behavioural and Biological Perspectives on the Origins of Modern Humans*. Princeton University Press, Princeton, pp. 232–244.
- Stringer, C.B., 1990. The emergence of modern humans. *Scientific American* December, 98–104.
- Stuut, J.-B.W., Prins, M.A., Schneider, R.R., Weltje, G.J., Jansen, J.H.F., Postma, G., 2002. A 300-kyr record of aridity and wind strength in southwestern Africa: inferences from grain-size distributions of sediments on Walvis Ridge, SE Atlantic. *Marine Geology* 180, 221–233.
- Svendsen, J., Astakhov, V., Bolshiyakov, D., Demidov, I., Dowdeswell, J., Gataullin, V., Hjort, C., Hubberton, H., Larsen, E., Mangerud, J., Melles, M., Moeller, P., Saarnisto, M., Siegert, M., 1999. Maximum extent of the Eurasian ice sheets in the Barents and Kara Sea region during the Weichselian. *Boreas* 28, 234–242.
- Swezey, C., 2001. Eolian sediment responses to the Late Quaternary climate changes: temporal and spatial patterns in the Sahara. *Palaeogeography, Palaeoclimatology, Palaeoecology* 167, 119–155.
- Tchernov, E., 1992. Eurasian-African biotic exchanges through the Levantine corridor during the Neogene and Quaternary. *Courier Forschungs-Institut Senckenberg* 153, 103–123.
- Thomas, M.F., Thorp, M.B., 1995. Geomorphic responses to rapid climatic and hydrologic change during the late Pleistocene and early Holocene in the humid and sub-humid tropics. *Quaternary Science Reviews* 14, 193–207.
- Trinkaus, E., Duarte, C., 2003. The hybrid child from Portugal. *Scientific American* 13, 32–33.
- Valladas, H., Reyss, J.L., Joron, J.L., Valladas, G., Bar-Yosef, O., Vandermeersch, B., 1988. Thermoluminescence dating of Mousterian Proto-Cro-Magnon remains from Israel and the origin of modern man. *Nature* 331, 614–616.
- Vartanyan, S.L., Garutt, V.E., Sher, A.V., 1993. Holocene dwarf mammoths from Wrangel Island in the Siberian Arctic. *Nature* 362, 337–340.
- Vavrus, S.J., 1999. The response of the coupled Arctic sea ice–atmosphere system to orbital forcing and ice motion at 6 ka and 115 ka BP. *Journal of Climate* 12, 873–896.
- Volkel, J., 1989. Formation of dunes and pedogenesis as paleoclimatic indicators in the eastern part of the Republic of Niger (Sahara and Sahel). *Palaeoecology of Africa* 20, 37–54.
- Walter, R.C., Buffler, R.T., Bruggemann, J.H., Guillaume, M.M.M., Berhe, S.M., Negassi, B., Libsekal, Y., Cheng, H., Edwards, R.L., von Cosel, R., Néraudeau, D., Gagnon, M., 2004. Early human occupation of the Red Sea coast of Eritrea during the last interglacial. *Nature* 405, 65–69.
- Wang, P., 1999. Response of Western Pacific marginal seas to glacial cycles: paleoceanographic and sedimentological features. *Marine Geology* 156, 5–39.
- Weaver, A.J., 2004. The UVic Earth System Climate Model and the thermohaline circulation in past, present, and future climates. In: Stephen, R., Sparks, J., Hawkesworth, J.C. (Eds.), *State of the Planet: Frontiers and Challenges in Geophysics*. Geophysical Monograph Series 150. American Geophysical Union, Washington, DC, pp. 279–296.
- Weaver, A.J., Eby, M., Fanning, A.F., Wiebe, E.C., 1998. Simulated influence of carbon dioxide, orbital forcing and ice sheets on the climate of the last glacial maximum. *Nature* 394, 847–853.
- Weaver, A.J., Eby, M., Wiebe, E.C., Bitz, C.M., Duffy, P.B., Ewen, T.L., Fanning, A.F., Holland, M.M., MacFadyen, A., Matthews, H.D., Meissner, K.J., Saenko, O., Schmittner, A., Wang, H., Yoshimori, M., 2001. The UVic Earth System Climate Model: Model description, climatology and application to past, present and future climates. *Atmosphere-Ocean* 39, 361–428.
- Weaver, A.J., Saenko, O.A., Clark, P.U., Mitrovica, J.X., 2003. Meltwater Pulse 1A from Antarctica as a trigger of the Bölling–Allerød warm interval. *Science* 299, 1709–1713.
- White, J.W.C., 1993. Don't touch that dial. *Nature* 364, 186.
- Williams, M.A.J., Adamson, D.A., Williams, P.M., Morton, W.H., Parry, D.E., 1980. Jebel Marra Volcano: a link between the Nile Valley, the Sahara and Central Africa. In: Williams, M.A.J., Faure, H. (Eds.), *The Sahara and the Nile. Quaternary Environment and Prehistoric Occupation in Northern Africa*. Balkema, Rotterdam, pp. 305–337.
- Yoshimori, M., Reader, M.C., Weaver, A.J., MacFarlane, N.A., 2002. On the causes of glacial inception at 116 ka BP. *Climate Dynamics* 18, 383–402.
- Yurtsev, B.A., 2001. The Pleistocene “tundra-steppe” and the productivity paradox: the landscape approach. *Quaternary Science Reviews* 20, 165–174.
- Zazula, G.D., Froese, D.G., Schweger, C.E., Mathewes, R.W., Beaudoin, A.B., Telka, A.M., Harington, C.R., Westgate, J.A., 2003. Ice-age steppe vegetation in east Beringia. *Nature* 423, 603.